Experimental and numerical analysis of the shear nonlinear behaviour of Nomex honeycomb core: Application to insert sizing

Juan de Dios Rodriguez-Ramirez, Bruno Castanie*, Christophe Bouvet

Institut Clément Ader (ICA), Université de Toulouse, CNRS UMR 5312-INSA-ISAE-Mines Albi-UPS, Toulouse, France

Keywords:
Honeycomb
Shear testing
Buckling
Finite elements
Inserts

A B S T R A C T

This work is a contribution to the understanding of the nonlinear shear behaviour caused by cell postbuckling in Nomex honeycomb cores. First, an experimental benchmark study was made of different designs for the shear testing of honeycomb cores. Then, several test specimens were fabricated and tested, a 3D DIC system being used to measure and record the displacements. An Artificial Neural Network (ANN) was also used to identify the onset of bucking and collapse of the cells. The influence of the overall boundary conditions of shear tests on the buckling of the cells is presented both experimentally and numerically. The reversibility and test procedure results suggest that it may be possible to allow the shear strength to be increased by up to 35% under certain conditions.

1. Introduction

Sandwich structures are widely used for applications in a variety of domains, such as the aerospace, naval, civil, and automotive fields, for acclimated transportation, aircraft parts, fluid storage, embedded electronics, etc.

These structures offer exceptional benefits when they are used in aeronautics. The incorporation of this technology into aircraft structures has proved to provide an excellent solution to mass reduction problems thanks to the resulting high bending stiffness and low weight, which allows lightweight parts to be designed. Nevertheless, as far as primary structures are concerned, honeycomb cores have so far been restricted to helicopter structures and to some business jets [1–3] but they are widely used for secondary structures in civil aviation. Most of the core used, e.g. for cabin interiors or landing gear doors, is made of Nomex honeycomb [4–7]. It is well known that, when a sandwich is subjected to a bending load, the core absorbs almost all the shear components of the force. Consequently, the shear properties of the core are very important for the sandwich design. Nevertheless, these properties are not as simple to determine as it may seem because the honeycomb core is a cellular structure and not a solid material.

Various tests are available for obtaining the shear properties of a honeycomb core, such as three and four point beam flexure (ASTM C393), double- and single-lap shear tests (the latter is normalized in the ASTM C273 [8]), or variants such as the method for testing thick honeycomb composites developed by NASA. However, the rail shear test is the most commonly used method. Such tests should provide very similar responses for the elastic characteristics of a given core. Nevertheless, the response may be affected by the thickness of the core and correcting factors need to be applied [9–11].

There have been several investigations of the nonlinear behavior of honeycomb cores. In the related literature, the main topic is clearly the compressive response, a phenomenon that has been studied for a long time (see McFarland since 1965 [12] or Wierzbicki [13]). Many authors have studied the compressive behavior - mainly to analyse the energy absorbing capabilities of honeycomb ([12–17] for example) or, more precisely, the crush behavior of the core after a low-velocity/low-energy impact on a sandwich [17–24]. Today, the tendency is to use very refined finite element analysis with explicit code to model the complex failure mode following crushing of the Nomex Honeycomb core.

However, by understanding the structural behavior of the hexagonal cell and by making an analogy with the postbuckling of stiffened structures [22], it is possible to propose simplified discrete models that are very accurate [22–24].

There are far fewer studies concerning the nonlinear behavior of honeycomb in shear. In 1992, Zhang and Ashby [25] stated that “The linear-elastic regime terminates when the cell walls of the honeycombs buckle elastically or bend plastically, or fracture in a brittle manner” but, for low density honeycombs as in the case of Nomex, it is the buckling that explains the nonlinear response. Zhang and Ashby then developed an analytical model based on the buckling formulas of the plates, which allowed shear collapse stress to be calculated but did not investigate the nonlinear domain itself. They also underlined the experimental difficulties related to the fact that it is impossible to test

* Corresponding author.
E-mail address: bruno.castanie@insa-toulouse.fr (B. Castanie).

https://doi.org/10.1016/j.compstruct.2018.03.076

honeycomb alone in pure shear. Pan et al. [26,27] analysed the shear buckling of aluminium honeycombs and proposed improved analytical methods for calculating the buckling load. Bianchi et al. [28] analysed the nonlinear responses of honeycomb made of aluminium in shear experiments and proposed finite element modelling with initial imperfections. The analysis also focused on their behavior in the orthotropic or off-axis directions. The model makes it possible to correctly predict the stiffnesses and the critical buckling load, which is considered here, as in previous publications, as the sizing load. Gornet et al. [29] analysed nonlinear shear behavior using a symmetrical shear test, but proposed a nonlinear model based on damage mechanics only in compression.

In fact, there are also studies on the nonlinear shear behavior of honeycombs by authors interested in the pull-out of inserts in sandwich structures [4], and this is also what motivated the present study. Bunyawanichakul et al. [5,6] propose a nonlinear model of highly loaded inserts that take the nonlinear honeycomb response, the nonlinear potting behaviour and the punching failure of the CFRP laminate skins into account. The nonlinear shear laws (τ vs γ) are obtained by a 3-point bending test and identification with a finite element model. Roy et al. [30], like Heimbs [31], model the exact geometry of the honeycomb to find nonlinear shear responses. However, the results depend on good determination of the material characteristics of the impregnated aramid paper used [32] and on whether the local geometry is properly taken into account. Seemann and Krause [4] have proposed a very detailed model of Nomex honeycomb that exhaustively considers the honeycomb defects and mesostructure and is able to model the nonlinear shear response with a rail shear test.

To sum up, the research effort on nonlinear shear behaviour of honeycomb remains limited and some results are questionable. For example, it can be seen that the buckling modes that occur during a rail shear test and those in proximity to inserts are very different, although the core is subjected to shear in both cases (Fig. 1). In particular, for the two parts of Fig. 1, the vertical cell edges remain straight near the insert whereas they buckle for the rail shear test. This means that the two honeycomb cores may show different structural behaviour and thus different failure scenarios. Similarly, the nonlinear shear behavior varies according to the authors; for example, the differences between the results obtained by Bunywanichakul et al. [5,6] and by Seeman and Krause [4] deserve to be explained. Finally, although many authors identify the shear buckling of honeycomb cells perfectly, no author has raised the question of the reversibility of postbuckling to date. Yet postbuckling is the basis for the design of aeronautical structures [33–35] that tolerate its reversibility without their strength being affected. Therefore, it would be possible, a priori, to consider not the critical buckling load but a non-reversible postbuckling threshold as the design load.

The present study reports a detailed experimental and numerical investigation of Nomex honeycomb core buckling and postbuckling under different boundary conditions through different types of tests.

2. Experimental study of the shear behaviour of HRH-78 under conventional boundary conditions

First, a benchmark study was made of the designs of specimens for the shear testing of honeycomb cores. Then, 12 specimens were tested, the tests being recorded by a 3D digital image correlation system (DIC). The data obtained were analysed to study the buckling of the cells. Finally, a detailed description was made of the nonlinear behaviour and buckling evolution of the cells.

2.1. Benchmark of specimen designs for shear testing of honeycomb cores

In this work, four different types of specimens were fabricated and tested to observe the advantages offered by each design for a study of the nonlinear shear properties of a honeycomb core. The aim was to select the most appropriate design for obtaining the curves of average shear stress vs. engineering shear strain (denoted by γ) under cyclic loading, and determining the shear modulus of the core and the shear strength of the core. The tests also had to allow us to observe the evolution of the nonlinear behaviour of the structure itself and the evolution of buckling in it, and, finally, had to give repeatable results. The double rail shear test described in ASTM C273 [8] was excluded from this study because of its inability to permit proper cyclic tests after buckling of the cells.

2.1.1. Benchmark test specimens: description

The specimens were fabricated using 20 mm thick HRH-78-3/16-3.0 Nomex honeycomb core. According to the manufacturer [37], the shear moduli were 24.13 MPa and 31.71 MPa for the W and L directions respectively. The shear strengths, using the correction factor given by the manufacturer, were 0.513 MPa and 0.785 MPa for the W and L directions respectively. For this first analysis, only one of each kind of specimen was made.

The first specimen to be tested, and thereafter used as a reference, was a sandwich beam in a three-point test (Fig. 2). This specimen was identical to those used by Bunyawanichakul et al. [5,6] to investigate the shear properties of the HRH-78 Nomex honeycomb core. Also, this type of testing was performed by Giglio et al. in Ref. [38]. When a load is applied to this kind of sandwich beam, the core is subjected almost entirely to shear stresses as the skins absorb the flexural components. Therefore, tests of this type are very often used to determine the shear properties of honeycomb cores [39]. The core was oriented in the L direction and the skins where made of aluminium that was 2 mm thick. The specimens were 20 mm wide × 20 mm high × 160 mm long and the distance between the supports was 140 mm.

A double lap specimen (Fig. 3-a) was made and tested. As for the previous specimen, the core was subjected to shear stress while the flexural forces were dissipated by the symmetry of the specimen. The core was oriented in the W direction, the skins where made of 5 mm thick aluminium and each specimen was 15 complete cells long.

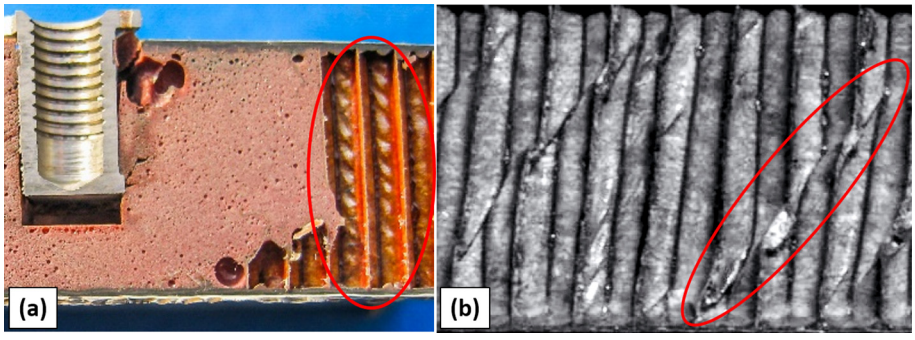

Fig. 1. Comparison of the buckling pattern of two Nomex honeycomb cores subjected to shear loads: (a) an insert specimen after a pull-out test where the cells have plasticized (extracted from Ref. [36]), versus (b) a single rail shear test (reproduced from Seemann et al. [4]).

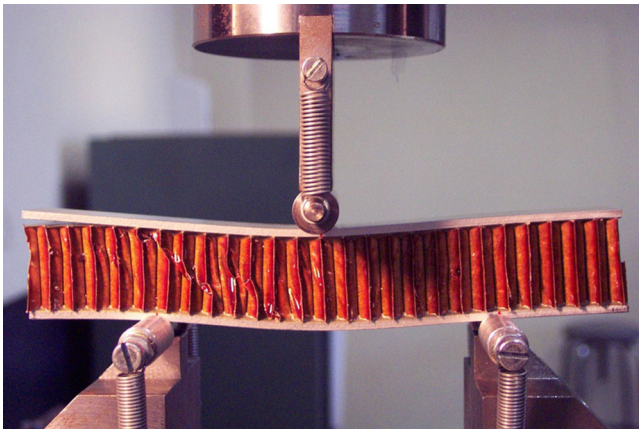

Fig. 2. Reference sandwich beam specimen under three point bending (reproduced from Ref. [36]).

A double single lap specimen (Fig. 3-b) was also fabricated and tested. This specimen was simple to make and subjected the core to both shear and flexural forces due to the thickness of the core. The same honeycomb core was oriented in the W direction, the skins were made of 5 mm thick aluminium to minimize the flexural deformations. The length of the specimen was 15 complete cells.

Another hybrid double lap specimen was fabricated and tested (Fig. 3-c). It was similar to the previous one but two materials were used instead of only the Nomex core. A specimen with similar characteristics has already been proposed by Hodge and Nettles in 1991 [40]. The purpose was to use a secondary material of greater stiffness in order to concentrate the shear forces on the desired section where the Nomex core was to be able to capture the shear buckling. The same honeycomb was tested in the L and W directions and the second material was plywood, also 20 mm thick. The skins were made of 5 mm thick aluminium.

For all the specimens, the cores were bonded to the skins with a redux 609 adhesive film and care was taken to avoid the glue filling the cells. Thus, several steps were needed to bond the cores to the skins perfectly.

2.1.2. Results and discussion

All specimens were tested using a 10 kN Instron machine. The force was directly measured from the machine and an external LDVT sensor was installed to measure the imposed displacement. A 3D-DIC system (VIC-3D) was used to measure the displacement field in and out and of the plane of the cells and the skins. The average shear stress was calculated by dividing the applied force between the projections of the area of the specimens. The shear angle (γ) was the relative displacement of the two skins (based on 3D DIC data) divided by the thickness of the core. The curves of all the test specimens are compared in Fig. 4. It is already important to emphasize that, although the responses in the linear domain are identical, the nonlinear part differs significantly from one type of trial to another. The ability of the tests to provide information on shear buckling of the cells is discussed in the following subsections.

The sandwich beam specimen (Fig. 2) was very simple to make but it was impossible to analyse its buckling very accurately. From a theoretical point of view using beam theory, the shear should be uniform in the core. However, this was no longer found to be the case when a refined FE analysis was performed [5,6] and the buckling was complex to analyse locally. The evolution of the buckling was measurable by the 3D-DIC system (Fig. 5-a) but the imposed displacement created some difficulties for measuring the displacement field of the cells. Thus, they had to be inspected one by one, which was not very practical. Also, the burr remaining after the cells were cut obstructed the visibility of the cameras. The failure of the specimen occurred by collapse of the cells on one side of the beam.

The double single lap specimens were simple to make but the results were not as expected. The effect of the flexural forces was very strong because of the shift of the neutral line, which generated a large out-of-plane deflection. Thus, the load-displacement curves obtained could not be used for the analysis of nonlinear shear behaviour (Fig. 4). The buckling of the cells was not uniform, as it began only at one side (see Fig. 5-b). This effect could have been avoided by adding articulations at each end of the specimen as was done by Seemann et al. [4] but this would have added some complexity to the fabrication procedure and test setup.

The best results, according to our criteria, were obtained with the double lap specimens. Also, the displacement field could be measured easily by the 3D-DIC system (see Fig. 5-c) as the buckling appeared randomly, due to initial imperfections in the honeycomb. On the other hand, failure could occur randomly on both sections of the test specimen, which posed a major problem.

For the two-material specimen, failure occurred in the honeycomb side, as expected, and the buckling of the cells was visible. However, the measured shear strength of the core was weaker than expected. The plywood did not allow a reduction of height of the honeycomb cells (see Fig. 15), because it was much stiffer in shear than the Nomex honeycomb core. Therefore, with this degree of freedom blocked, the buckling behavior of the cells was not uniform. In other words, because the two different materials produced different deformations in the thickness direction, there was a more complex stress state in the Nomex side and the interpretation of the experiment was more problematic.

In conclusion, all the specimens could be used to study the elastic shear properties of the core but the nonlinear behaviour and the failure scenarios were different. Moreover, thin face sheets were used for these tests, which meant that there was significant local face sheet bending due to the eccentric load paths. Consequently, the core did not experience a pure shear stress state and there were significant shear stress concentrations towards the ends of the Nomex core/facesheet bond lines, resulting in significant peeling stresses in these interfaces. So although simple, the tests proposed did not provide well defined or simple Nomex core stress or deformation states in the vicinity of the ends of the Nomex/face sheet interfaces. Thus none of the tests is

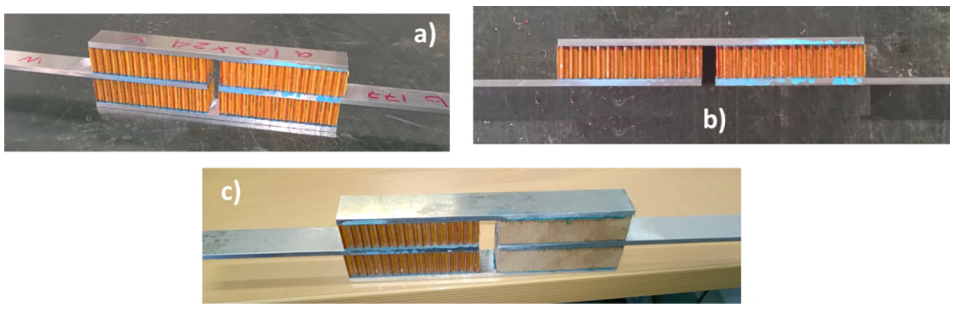

Fig. 3. Three different specimens benchmarked a) Double lap specimen; b) Double single lap specimen; c) Two material double lap specimen.

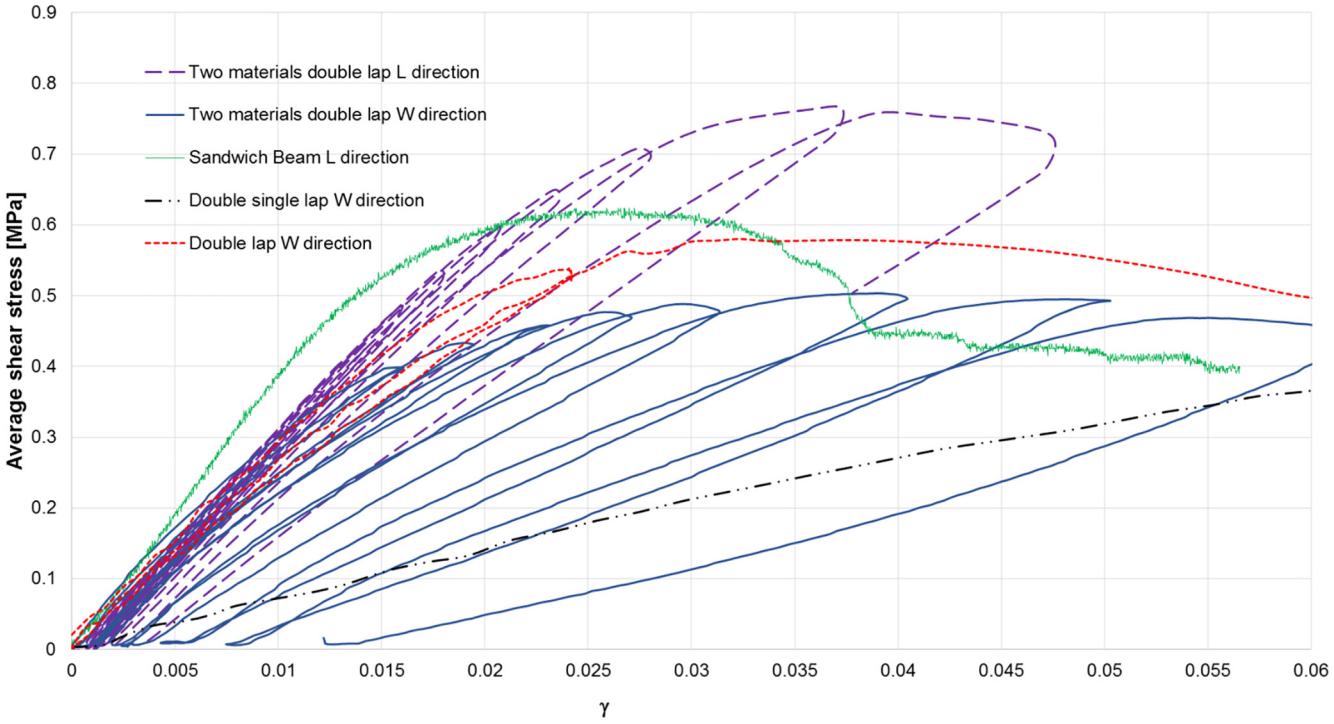

Fig. 4. Curves of average shear stress vs γ for each type of specimens.

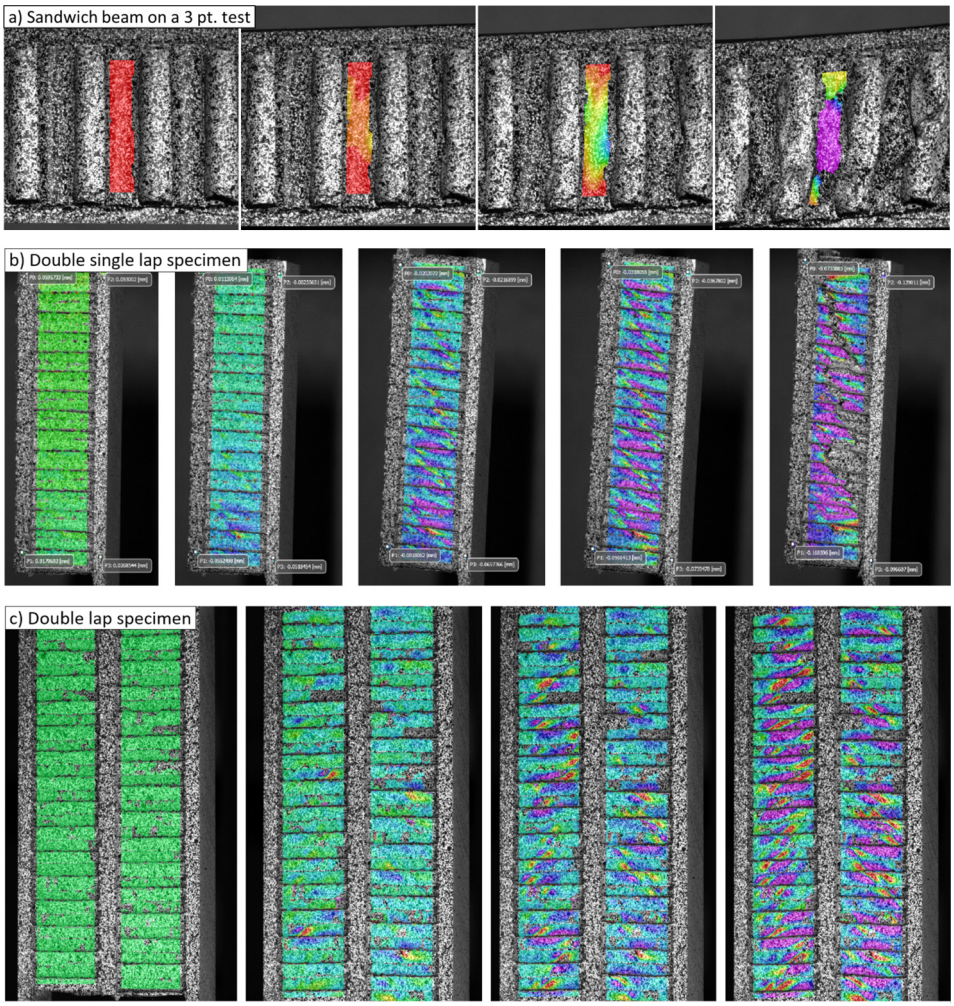

Fig. 5. Displacement field measured in the out-of-plane direction of a) the sandwich beam, b) the double single lap specimen, c) the double lap specimen.

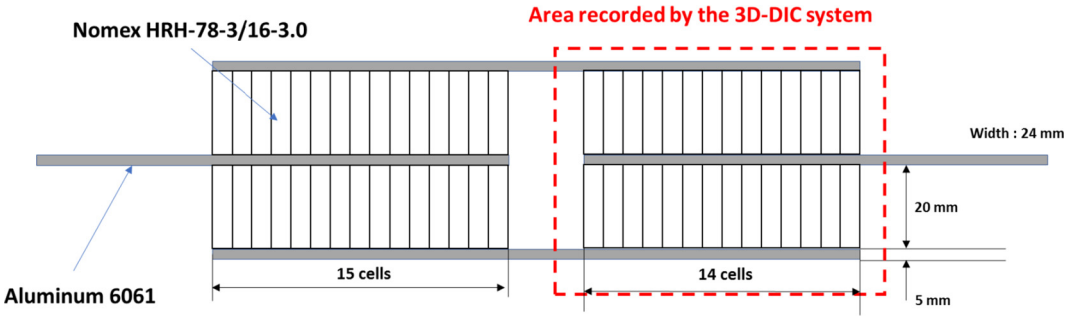

Fig. 6. Characteristics of the double lap specimen.

perfect. The beam and the single lap specimens were the easiest to make but more accurate results were obtained with the double lap specimens, and using the 3D-DIC system was easier and quicker. Considering these facts, the most suitable design for our research was the double lap specimen. To ensure that the failure of the specimen would appear in the side recorded by the 3D-DIC system (Fig. 5), the two pieces of Nomex of one side needed to be cut slightly shorter (e.g., minus one cell). This increased the average shear stress in that side and induced failure where it was desired without causing significant variation in the measurements.

2.2. Testing HRH-78

To continue the investigation, 12 new double lap specimens were made, six in the W direction and six in the L direction according to the dimensions shown in Fig. 6. One section was slightly shorter to induce failure in the section where the 3D-DIC system was recording the tests.

Two types of tests were performed. For both, the speed of the machine was set to 1 mm/s. In the first type, a continuous displacement was imposed to determine the overall shear response. In the second, an increasing cyclic displacement was imposed, which allowed the elastic postbuckling domain of the honeycomb structure to be analysed under shear forces. To obtain reliable results and check the reproducibility of the data, each experiment was reproduced three times. This resulted in a total of 12 specimens (2 directions × 2 types of test × 3 specimens). All specimens were tested using a 10 kN Instron machine. The procedure to calculate the average shear stress and γ was the same as that used in the benchmark study. The results are shown in Fig. 7.

After testing the first six specimens, it was found that the average shear moduli of the W and L directions were 25 MPa and 32 MPa, respectively, and the maximum shear stresses were, on average, 0.58 MPa and 0.76 MPa, respectively. These results are consistent with the data provided by the manufacturer [37]. The failure mode was the same for the 12 specimens. It began with an accentuated deformation of the smaller side, then there was a major collapse of only one piece of honeycomb, followed by collapse of the other one (Fig. 8).

The remaining six specimens were subjected to incremental cyclic displacements (Fig. 9). At each cycle, the maximum displacement imposed was increased slightly in order to be able to identify the stress and γ at which the honeycomb structure started to become damaged. As expected, hysteresis was only slight at the beginning. The cyclic tests revealed that there was a significant reduction of the stiffness once γ exceeded 0.0211 (0.52 MPa) in the W direction and $\gamma = 0.022$ (0.65 MPa) in the L direction. This could mean that, at this point, the deformations of the cells were severe enough to affect the behaviour of the honeycomb structure. Before this point, shear buckling probably occurred without damaging the phenolic resin at the surface of the cells and so the buckling was reversible. This point will be analysed more precisely in the following subsections.

2.3. Analysis of the buckling and postbuckling behaviour of the cells

The cells of the honeycomb core were weaker when they were tested in the W direction, because of the orientations and the thicknesses of the walls. For this reason, the refined analysis of the buckling of the cells is presented only for cases where the force was applied in the W direction. The 3D-DIC system allowed images to be created that represented the displacement field in the three directions, x, y and z with a colour scale, making it possible to look more closely at the evolution of buckling of the walls at the exterior surface of the test specimens. The cell walls were expected to buckle towards ± 30° from the plane of view of the cameras but, considering that the magnitude of the deformations should be very small, we assumed that measuring the deformations in the Z direction with respect to the cameras would be accurate enough. Determining a scale to measure buckling was complicated because the buckled shape was not necessarily the same in all the cells. Also, the magnitude of the buckling increased with increasing γ.

By inspecting the videos of the tests, we found that changing the analysis scale allowed different aspects of the buckles to be studied (see Fig. 10a) and b)). If the scale was set to measure the deformations out of the plane from 0 mm to 0.04 mm, it was observed that the shape of buckles grew but the deformations did not visibly propagate to the adjacent cells. Therefore, we assumed that they were not directly related to the collapse of the cells. If the scale was set to measure the deformations in the plane from 0 mm to −0.04 mm, the shape of the buckles was observed to grow, propagating buckling to the adjacent cells. Therefore, we assumed that the negative deformations were related to the collapse of the cells. The buckling was not symmetric – probably because of the boundary conditions of the outer cells.

Regardless of the scale, some buckles started to be clearly visible at an average shear stress of 0.24 MPa (Fig. 11). Also, the recorded images of the three specimens were inspected when the average shear stress was 0.4 MPa (Fig. 11), which is also where the nonlinear behaviour presumably started. We hypothesized that, at this point, the buckling occurred at sufficiently numerous places to affect the stability of the honeycomb, thus changing the loading slope. The maximum extent of buckling towards the inside of the plane was measured automatically by the VIC-3D software at the point where a stress of 0.4 MPa was applied to each specimen; the average value was −0.1054 mm. Considering the above information, the scale of the recorded videos of the three specimens was set between 0 mm and −0.1054 mm to measure the buckles. The resulting images can be seen in Fig. 12.

The buckles started as very small, isolated deformations. At a certain point, their shape grew and covered a significant area of the cell walls. Then, the buckles grew and propagated to the adjacent cells, causing the shear collapse of the edge and thus a more global collapse of the buckled cell and surrounding cells. We also observed that the cells did not necessarily collapse all at the same time.

The different stages of the nonlinear shear behaviour of the cells were thus identified as:

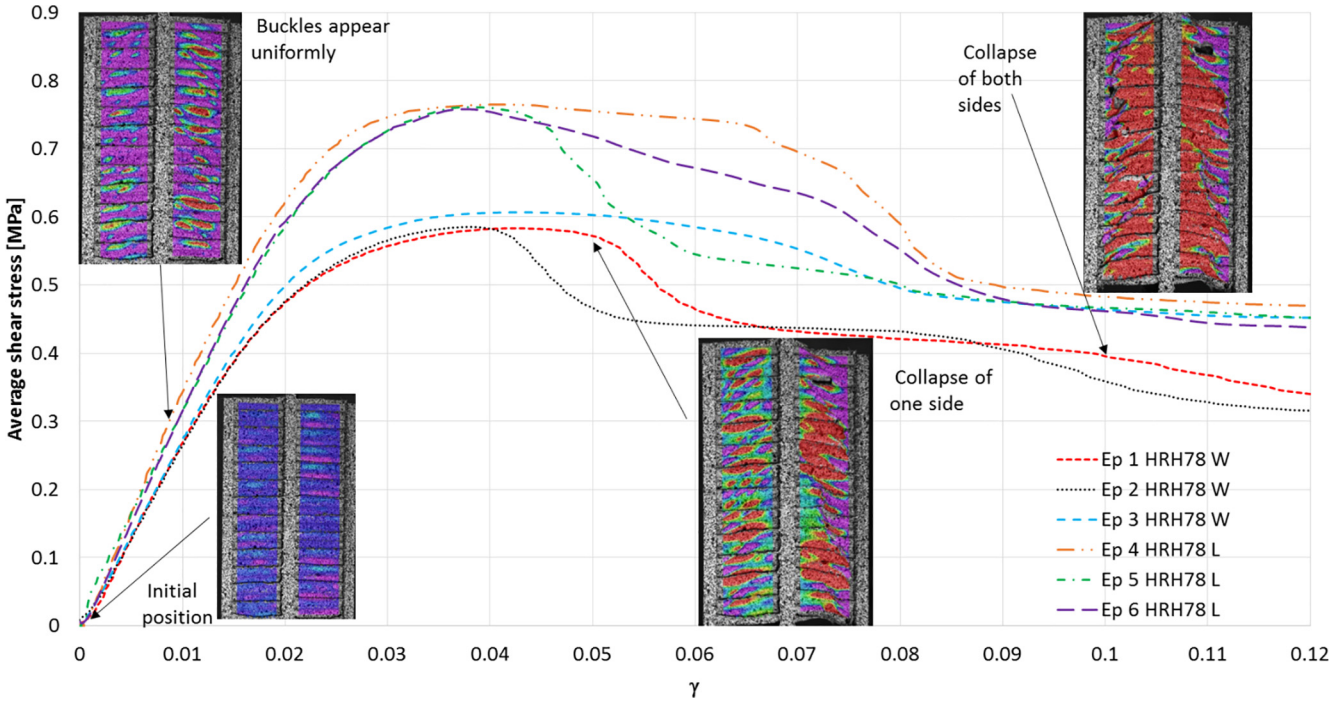

Fig. 7. Average shear stress vs γ curves of the HRH-78 in W and L direction.

- Initial buckling of the walls,
- Stable postbuckling with increase of the size of the buckles,
- Collapse of the cells due the buckling of the cell edge under shear and, finally, when the extent of buckling was large enough, propagation of the buckled shape to the adjacent cells, causing them to collapse.

It is noticeable that this scenario is very similar to the scenario of crushing identified by Aminanda et al. [22] and is typical of the behaviour of stiffened structures.

2.4. Collapse of the cells

A more detailed analysis of the collapse of the cells is necessary to identify when the cells start to collapse and how much influence this has on the global behaviour of the structure. This is not an easy task because the collapse can vary greatly from cell to cell.

Fig. 12 shows the evolution before the collapse of one cell. The buckles in red stop growing once the vertical edges of the cell are no longer straight at mid height. Thus the cell is about to collapse. We supposed that there could be a direct relation between the area of the buckle (red area) and the collapse of the cell. Therefore, monitoring the growth of the buckling could be a good method to detect when a cell was just about to collapse. To study the collapse of the cells of the specimens, 13,334 images needed to be analysed. Such complexity could lead to subjective inaccuracies if the analysis was performed by a human, so an artificial neural network (ANN) was developed to carry out the task. This reduced the analysis time while providing an objective method for detecting when cells were about to collapse.

The ANN was trained with 29 examples of cells that were about to buckle and 50 examples of non-buckled cells selected by the authors; some examples can be seen in Fig. 13. After the training, the ANN knew how to detect 29 different buckling patterns. This was very helpful because it enabled the ANN to detect the collapse of the cells almost regardless of the buckling pattern. Image preprocessing was performed on each frame of the videos. First, the cells were cut from all the frames of each video. Then all cell images where reshaped to the same number of pixels. After this, a colour segmentation filter was applied to focus the analysis on the red tone (the buckled parts). The ANN was used to analyse the images from the tests. The results are shown in Fig. 14. Both the left and right sides of the specimens were analysed. The analysis revealed that the nonlinear behaviour started before any cell was

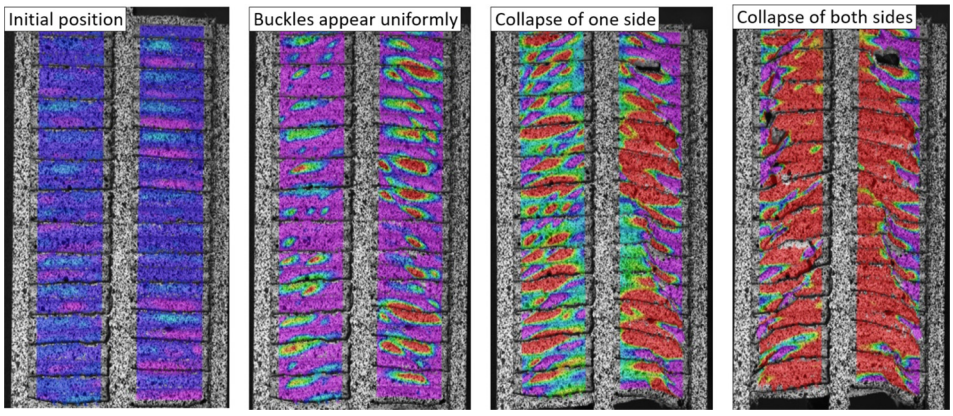

Fig. 8. Failure scenario of the double lap specimen.

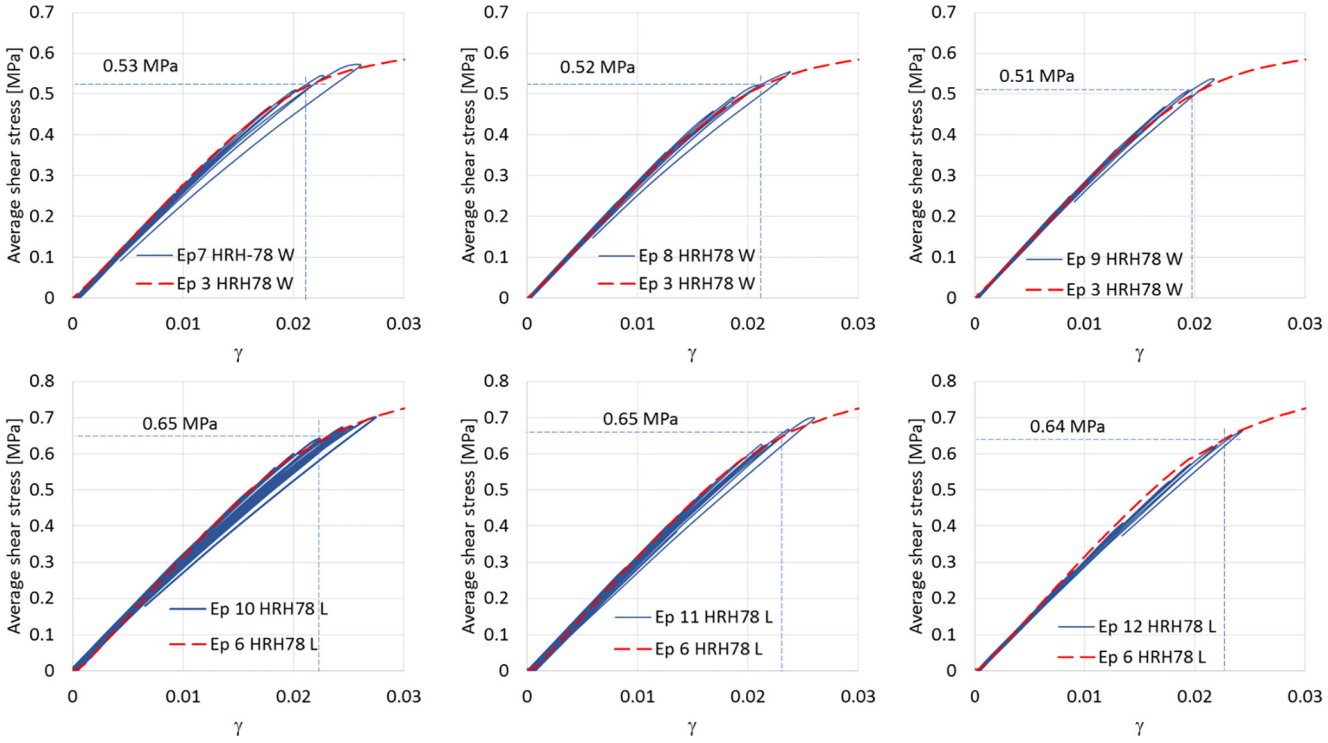

Fig. 9. Incremental cyclic testing on the HRH-78 core: average shear stress vs γ.

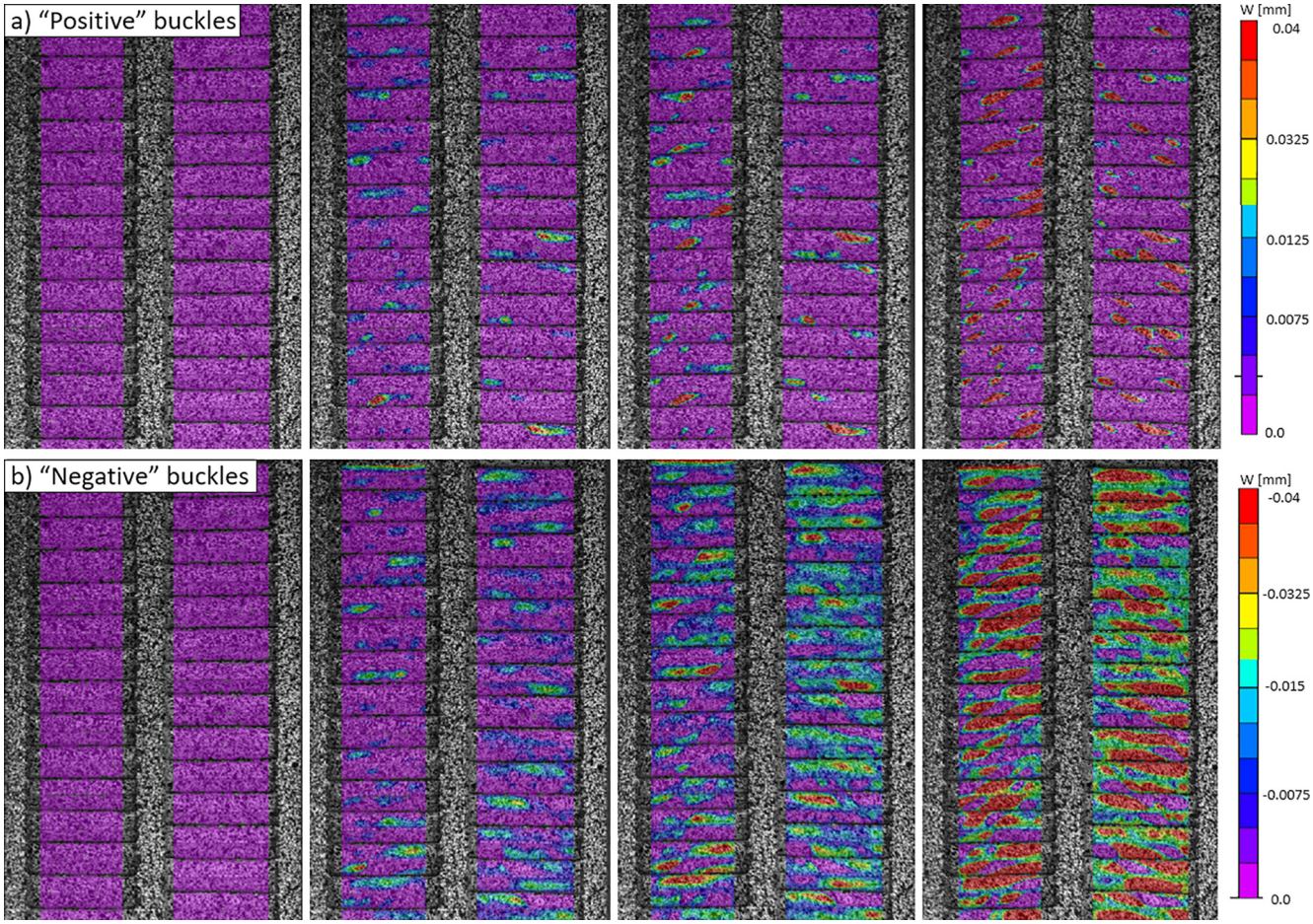

Fig. 10. Evolution of Z-displacements measured from a) 0 mm to 0.04 mm and b) 0 mm to −0.04 mm.

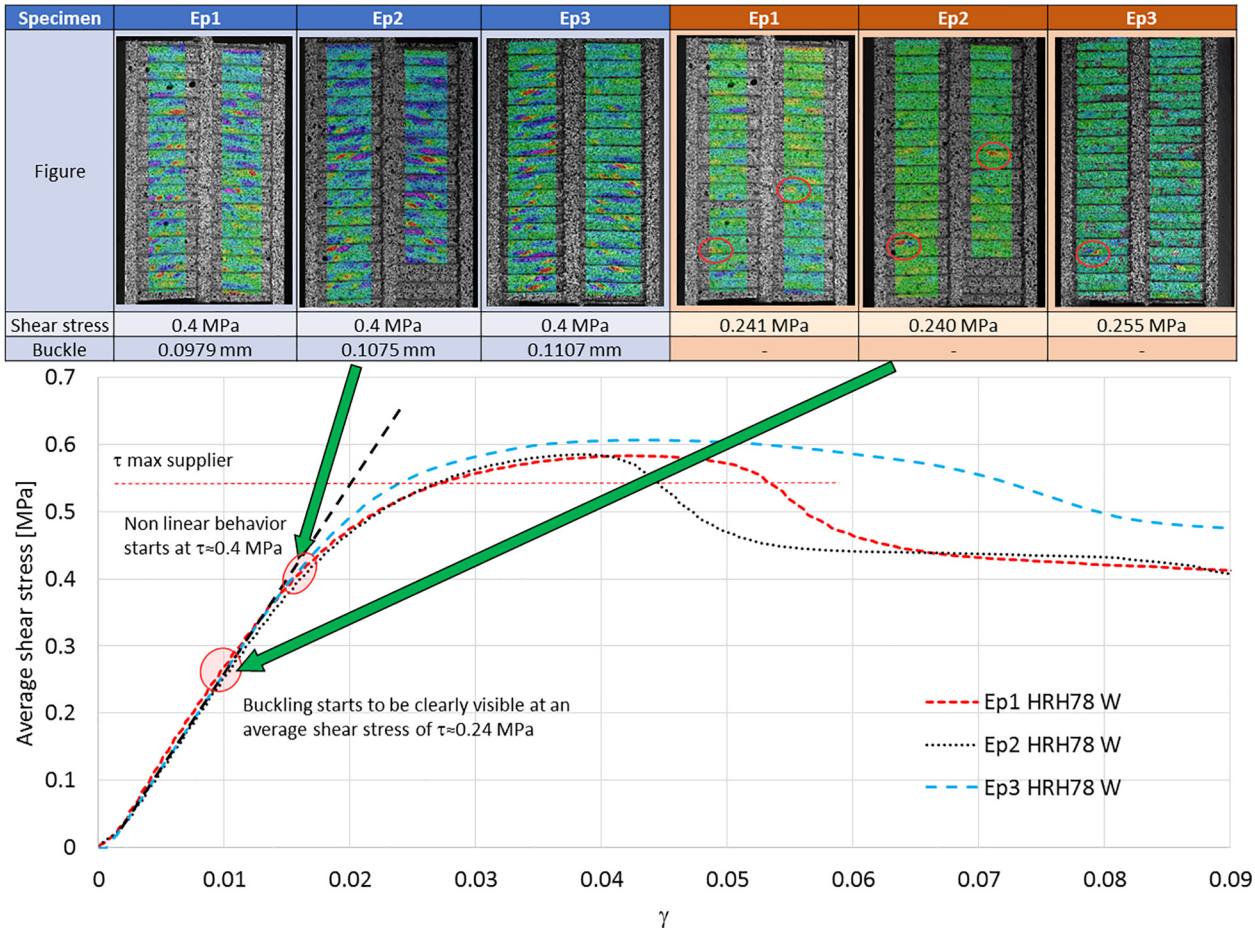

Fig. 11. Buckling of the cells at 0.24 MPa and 0.4 MPa.

detected as being about to collapse. This confirms that initial nonlinear behaviour of the curve is not related to the collapse of the cells but to the initial local buckling and stable postbuckling period.

2.5. *Conclusions of the experimental analysis*

The evolution of buckling of the HRH-78 Nomex honeycomb core in the double lap test considered here can be described as follows:

- From $\gamma = 0$ to $\gamma = 0.00845$ (0 MPa–0.24 MPa), the magnitude of the buckles is very small, almost undetectable. The overall behaviour of the honeycomb is linear elastic (see Fig. 11).
- From $\gamma = 0.00845$ to $\gamma = 0.01542$ (0.24 MPa–0.4 MPa), the buckles start to be clearly visible and affect the linear behaviour of the honeycomb structure very slightly. The cell walls buckle progressively. The honeycomb structure works in a reversible postbuckling regime. The overall behaviour of the honeycomb is still elastic (see Fig. 11).
- From $\gamma = 0.01542$ to $\gamma = 0.01822$ (0.4 MPa–0.46 MPa), the average shear stress vs. γ curve indicates more visible nonlinear behaviour. The incremental cyclic tests presumably indicate that the honeycomb structure remains elastic with no hysteresis (see Fig. 9). The honeycomb structure still works in a reversible postbuckling regime. The overall behaviour of the honeycomb is nonlinear elastic.
- From $\gamma = 0.01822$ to $\gamma = 0.02151$ (0.46 MPa–0.52 MPa) the buckles have propagated enough to cause instability of some cells, which start to collapse (see Fig. 14). However, the incremental cyclic test indicates that the structure remains elastic (see Fig. 9). This could

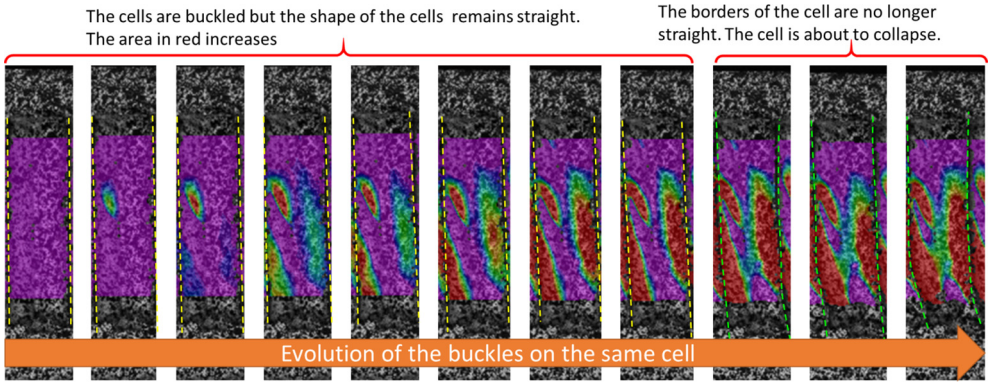

Fig. 12. Buckling evolution of a cell: from initial buckling to collapse.

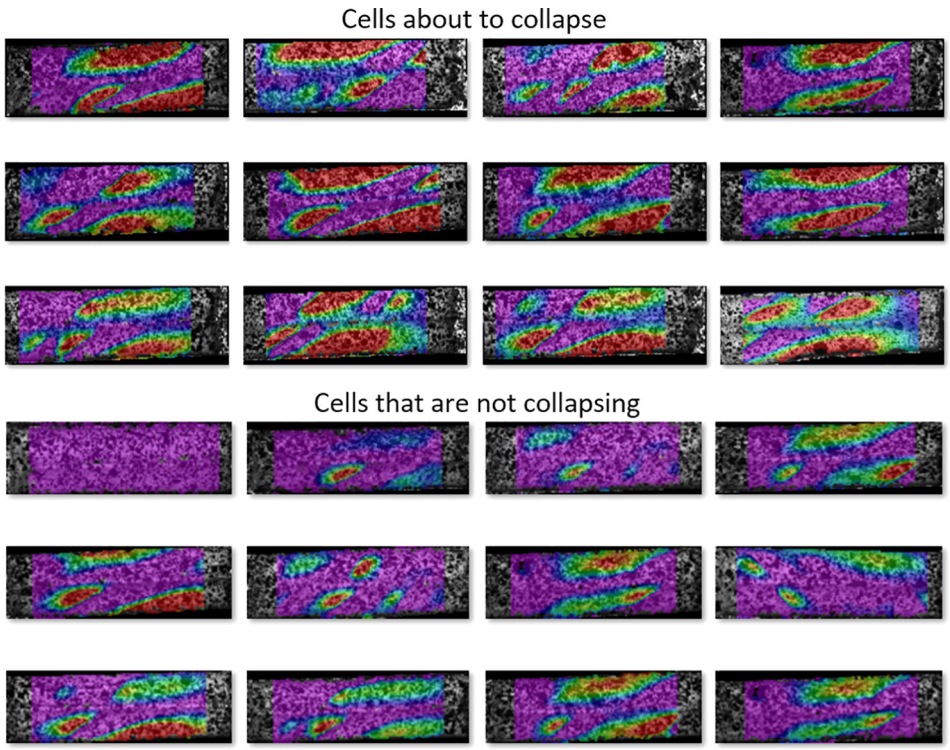

Fig. 13. Examples of collapsing and non-collapsing cells to train the ANN.

mean that the buckling of the Nomex paper was still elastic or that the overall deformations were very small or not large enough to cause significant damage of the structure.

- From $\gamma = 0.02151$ to $\gamma = 0.03$ (0.52 MPa–0.59 MPa), the cyclic test indicates that the structure is permanently damaged (see Fig. 9). The deformation of the cells propagates and they continue to collapse. The maximum average shear stress is presumably reached when the last cell is about to collapse (see Fig. 14). At this point, the Nomex paper tears in some areas.

Considering the above analysis, it can be said that the nonlinear behaviour of the honeycomb in shear is related to two different phenomena. It begins with the apparition of local buckles in the cells, which cause a slight loss of stiffness. Then, the cells collapse, causing a major loss of stiffness of the structure (see Fig. 10). When all the cells have collapsed, it would be logical for the shear stress to decrease.

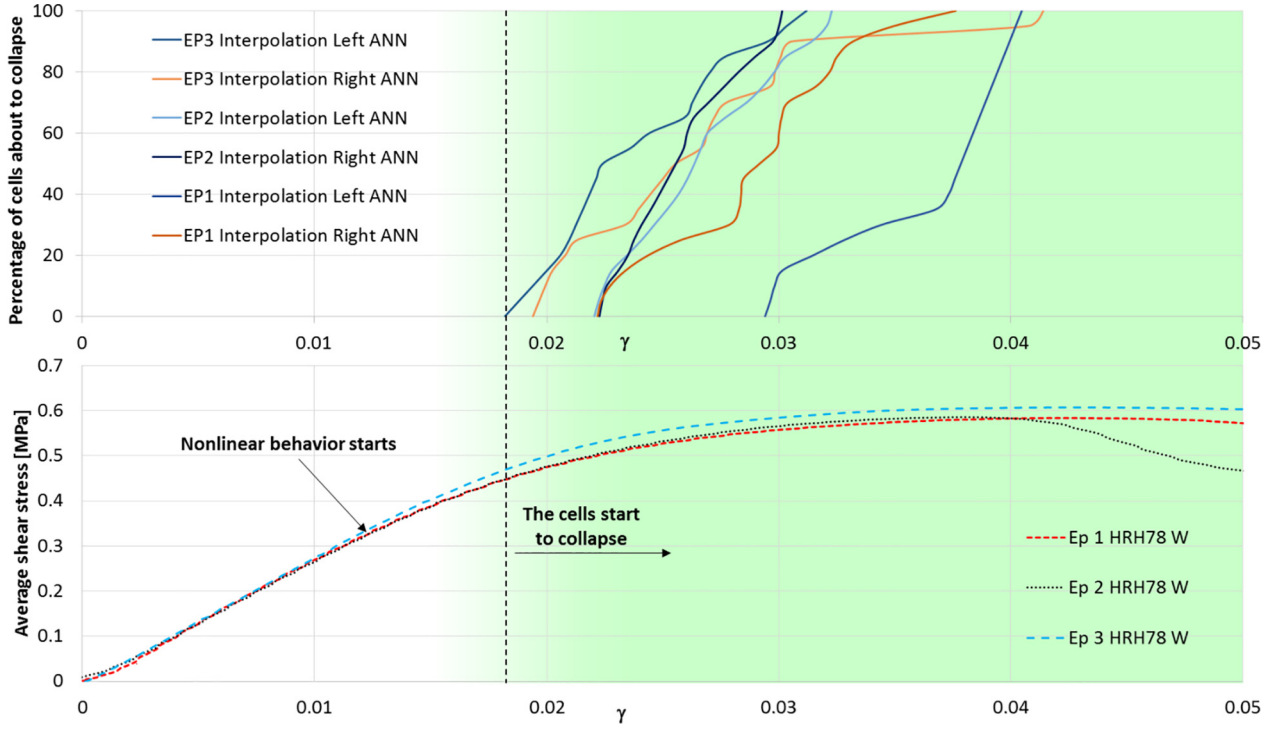

Fig. 14. Collapse of the cells, according to the results given by the ANN, vs the average shear stress.

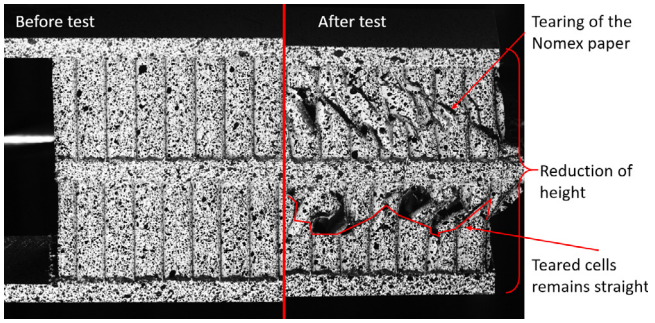

Fig. 15. Comparison of a specimen before and after the test.

However, the analysis detected that all the cells were already collapsing at approximately $\gamma = 0.04$ while the measured shear stress was still $\tau = 0.5$ MPa, which suggests that the collapse is slow and gradual, not dramatic. Also, once the cells have collapsed, if the displacement of the skins continues to increase, the cells start to break at approximately $\gamma = 0.06$. After this they are no longer inclined (see Fig. 13), so this residual strength can be attributed to the breaking and tearing of the paper of the honeycomb cells.

3. Numerical study of shear buckling of cells

The experimental study revealed that the onset of buckling of the cells appeared at relatively low shear stresses. When the honeycomb was subjected to shear loads, it initially showed linear behaviour that could be described with a shear modulus. If the stress was increased further, the slope of the curve changed. Our research suggests that at least two different phenomena are involved in the nonlinear behaviour of the honeycomb in shear. Presumably, local buckling initiates the nonlinear behaviour. Then, after a postbuckling period, the collapse of the cells causes the final degradation of the shear modulus. These ideas are very similar to the conclusions of Aminanda et al. in Ref. [22]: when they studied the buckling of Nomex cells under compression, they concluded that the change of behaviour was caused by the buckling of the cells in a stable configuration. Other interesting work was done by Roy et al. [32] as part of research concerning inserts. They created an FE model in order to identify the critical load of the honeycomb core and predicted the critical load under compression by measuring the rotation of the nodes of the FE model. This allowed a 2D chart to be drawn, identifying the force that made the honeycomb cells buckle.

In the present work, several FE models of the 20 mm thick HRH-78-3/16-3.0 honeycomb were created using Abaqus implicit. The implicit solver was chosen here because the loading was quasi static and only the geometric nonlinear behaviour was studied. These models helped to analyse the initiation of buckling under shear loadings. Also, an analysis of the shear stress vs the nodal rotation of the elements was performed to investigate the shear stability of the honeycomb cells.

3.1. Modelling the HRH-78 Nomex honeycomb core

3.1.1. Properties of Nomex paper

Nomex paper is made of aramid fibres. There are several types of Nomex papers and they are used for several applications. Nomex honeycomb core is created by the expansion of glued layers of Nomex paper, then the honeycomb is dipped in phenolic resin and finally cured. This increases its fire resistance, stiffness and density, as explained in Ref. [37]. The mechanical properties of Nomex papers have been studied by several authors. Tsujii et al. [41] did experimental work on this material. Foo et al. [42] performed tension tests on the paper without the phenolic resin coating, showing that the Nomex paper by itself is similar to an orthotropic material that presents significant plastic behaviour and allows considerable strains before breaking. Plasticity starts at 24 MPa and 40 MPa in the transversal and fibre directions, respectively, and the paper breaks at strains of 0.13 and 0.15 in the transversal and fibre directions, respectively. Roy et al. [32] performed tension tests on Nomex T-410 paper with and without the resin coating layer and showed that, when the coating layer was applied, the Nomex paper became stiffer and brittle, the plastic behaviour becoming almost insignificant. The resin layer was very thick and the tests were therefore not very representative. Breaking of the paper/resin occurred at 22.5 MPa and 40 MPa in the transversal and fibre directions, respectively. Fischer et al. [43] performed tension and compression tests on an aramid paper pre-impregnated with phenolic resin that was considered to be very similar to Nomex paper. They showed that the paper presented different plastic behaviour in compression and tension. Plasticity started at 40 MPa and 60 MPa in the transversal and fibre directions, respectively, when the paper was subjected to tension. In compression, on the other hand, plasticity started at 30 MPa for both transversal and fibre directions. Seemann et al. [4] directly asked the manufacturer, DuPont, for the mechanical properties of Nomex T-412 paper. These properties were very similar to those reported by Foo et al. and Roy et al. for T-410. They also proved that modelling the Nomex paper/phenolic resin walls as an isotropic material with perfect plasticity behaviour gave accurate results. However, this approach did not allow the abrupt failure of the honeycomb cells to be captured. According to the manufacturer, the HRH-78 Nomex honeycomb core is made of the Nomex commercial grade paper T-722, which is not recommended for aerospace applications [44]. Bitzer reports that the mechanical properties of T-722 are slightly lower than those of T-412 and that T-722 is not recommended for aerospace applications because this paper does not satisfy the FAR 25.853 flammability afterglow requirement [45].

Considering that the phenolic coating strongly modifies the mechanical properties of the aramid paper and assuming that the mechanical properties of T-722 and T-412 are very similar, since the exact mechanical properties of the T-722 Nomex paper were not available, in this study, we considered the mechanical properties of T-722 to be very similar to those of T-412 and T-410 Nomex papers when they are coated with phenolic resin. Also, to simplify the modelling of the coated Nomex paper, it was considered as a homogeneous isotropic material having a Young's modulus of 4000 MPa with perfect plasticity starting at 64 MPa. These assumptions were made after several attempts to correlate the experimental results. The selected values are also consistent with the recommendations of Seemann et al. in Ref. [4] for the homogenized modelling of T-412 coated paper. The only difference concerns the plastic behaviour, which, according to Seemann, should occur around 90 MPa. However, given that the material used here was not exactly the same, the model was assumed to be sufficiently representative.

3.1.2. Model features

Seemann et al. [4] made a very detailed study of how imperfections of the hexagonal geometry in Nomex honeycomb cores should be considered. They stated that taking the curved hexagon geometry into account was not to be recommended. Also, they indicated that considering irregular hexagon geometry produced results that were only 10% more accurate than those for the regular hexagon geometry. In the present work, the cell was taken to be a perfect hexagon with a cell diameter of c = 4.7625 mm. The difference of thickness of the single and double walls was taken into account; they were 0.06 mm and 0.12 mm thick respectively. The imperfections of the hexagonal cells were not considered. The model consisted of only 8 honeycomb cells. Only S4R shell elements were used and the approximate global size of the elements was 0.27 mm. The material of the cells was taken to be isotropic; it represented the paper and the phenolic resin coating layers as being homogenized. The bottom of the cells was fixed in displacement and rotation and the top was fixed in a similar way except that displacements in the Z and X directions were allowed (see Fig. 16).

No symmetry conditions were imposed on the exterior borders of

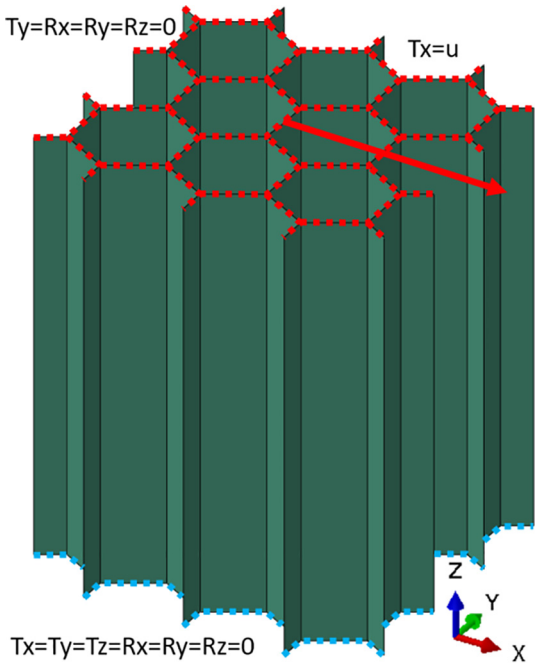

Fig. 16. Boundary conditions of the double lap test model.

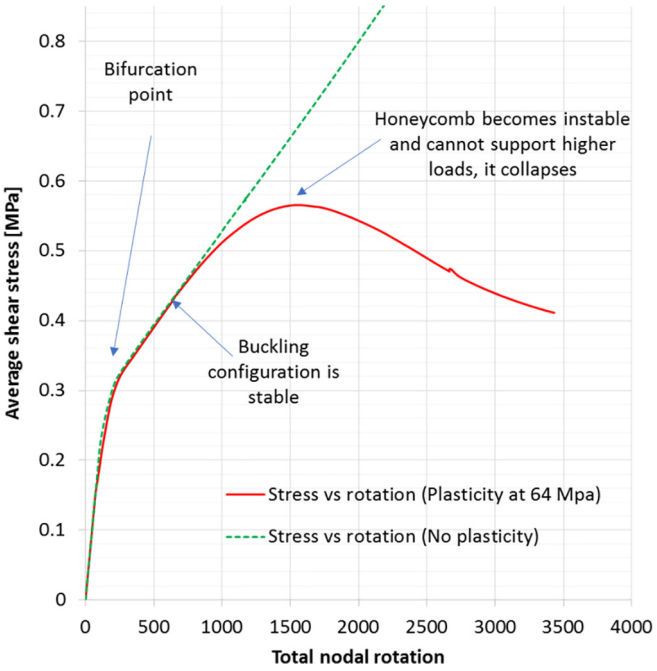

Fig. 18. Average shear stress vs nodal rotation of the double lap F.E. model.

the cells. First, a buckling analysis was performed to determine the buckling modes of the structure. Then, some buckling modes were incorporated into the model as initial imperfections in order to make a postbuckling analysis of the structure. Also, to determine whether the plasticity of the buckles had any notable influence on the overall shear behaviour of the honeycomb structure, two simulations were run: one considering plastic behaviour and the other non-plastic behaviour of the Nomex paper.

3.2. Results and discussion

No tearing of the Nomex paper was considered in the model, so the FE model was not representative beyond approximately $\gamma = 0.055$, i.e. the value at which tearing of the paper was detected in the experimental results. To compare the buckles in the F.E. model and the real tests, the colour scale of the F.E. model was set to be the same as the one used in the analysis of the experimental results (0 mm to −0.1024 mm). The numerical simulations of the shear test showed good correlation with the real tests. The buckling pattern of the cells was very similar, as were the shear curves (Fig. 17).

To analyse the buckling stability of the cells, it is necessary to find a way to measure the buckles of the cell walls. One way to do this could be to measure the rotations of the nodes of each wall but this would hardly be practical since buckling of the cells may occur in any direction. We decided that the best method was to obtain the sum of the rotations of all the nodes in every direction. This would give us a

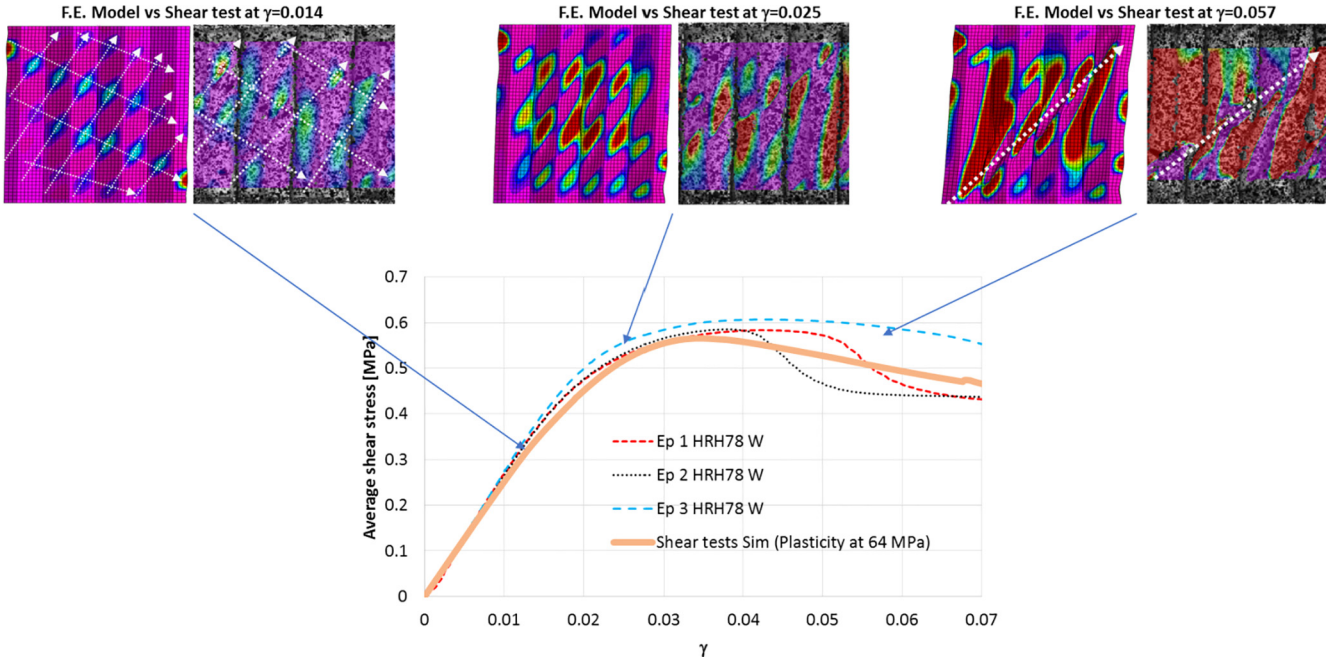

Fig. 17. Real tests vs simulation of HRH-78.

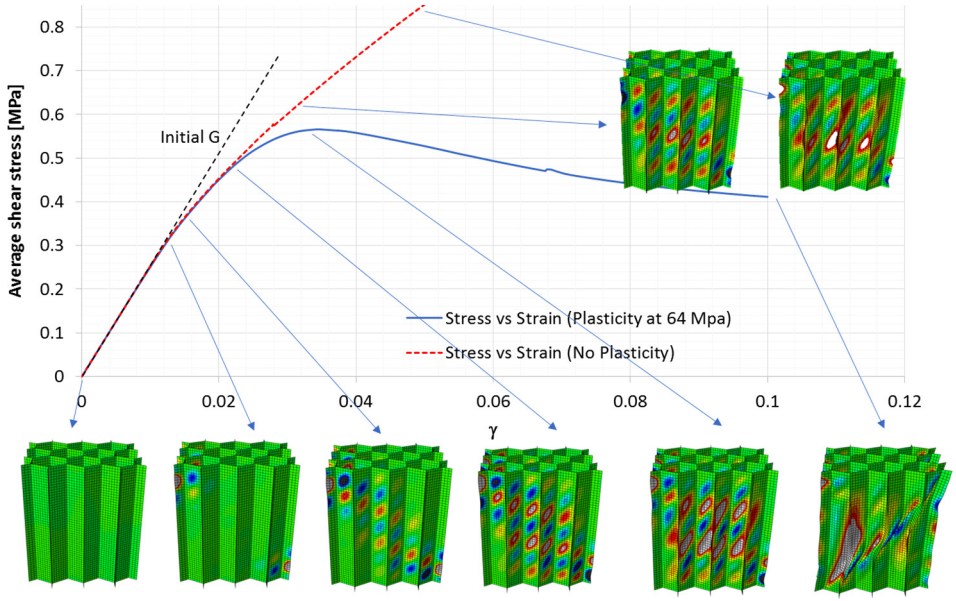

Fig. 19. Average shear stress vs γ for the double lap F.E. model.

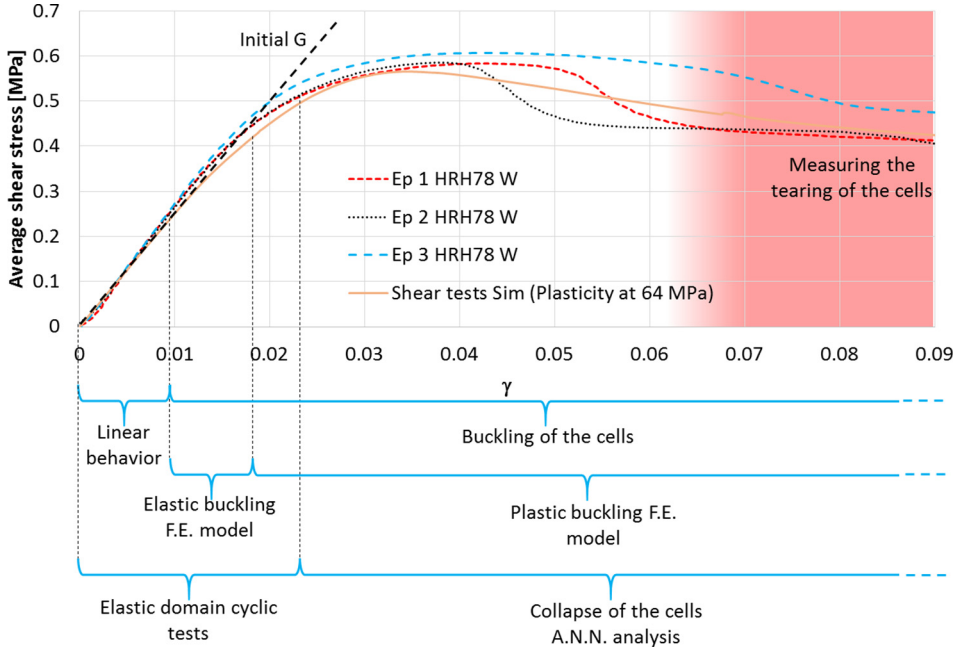

Fig. 20. Description of the nonlinear behaviour of the Nomex honeycomb core HRH-78.

general estimation of the start of buckling in the F.E. model and any abrupt change in this quantity would mean that the buckling configuration of the cells had changed. Fig. 18 shows the average shear stress vs the total nodal rotation. A bifurcation point can be detected at 0.31 MPa, corresponding to the onset of buckling. After this, the rotations of the nodes are seen to increase with the shear stress, meaning that this buckling configuration is stable. Finally, the cells collapse at 0.56 MPa. Also, when no plasticity for the material of the Nomex paper was considered in the F.E. model, the cells did not collapse. This means that the collapse of the cells was caused by the degradation of the Nomex paper and, therefore, that the stability of the cells may be attributed to the geometry of the cell that buckles into a stable configuration. In this way, it can be said that two phenomena take place when the honeycomb is crushed. First, the postbuckling of the cells in a stable configuration, and then the collapse of the cells because the material plasticizes and the edges fail. Also, by comparing the curves as shown in Fig. 19, we noticed that, in the F.E. model, even though the buckled areas started to plasticize at $\gamma = 0.018$ (0.42 MPa), the two curves were similar until $\gamma = 0.024$ (0.48 MPa).

The F.E. model allowed us to determine that the initial nonlinear behaviour of the shear stress vs γ curve was only related to the stable buckling of the cells. The paper started to plasticize when the honeycomb reached $\gamma = 0.018$, but the cyclic tests indicated that the global behaviour of the structure was not affected until $\gamma = 0.021$, which indicates that the buckled areas may plasticize without affecting the global behaviour of the structure. The analysis of the nonlinear behaviour of the honeycomb cells under shear stress is summed up in Fig. 20. Despite its relative simplicity and some discrepancy between experiment and numerical analysis, the model is able to correctly represent the nonlinear behaviour of the honeycomb in shear and so is acceptable for use. In the next section, it will be implemented to elucidate the point highlighted in the introduction (Fig. 1) concerning the

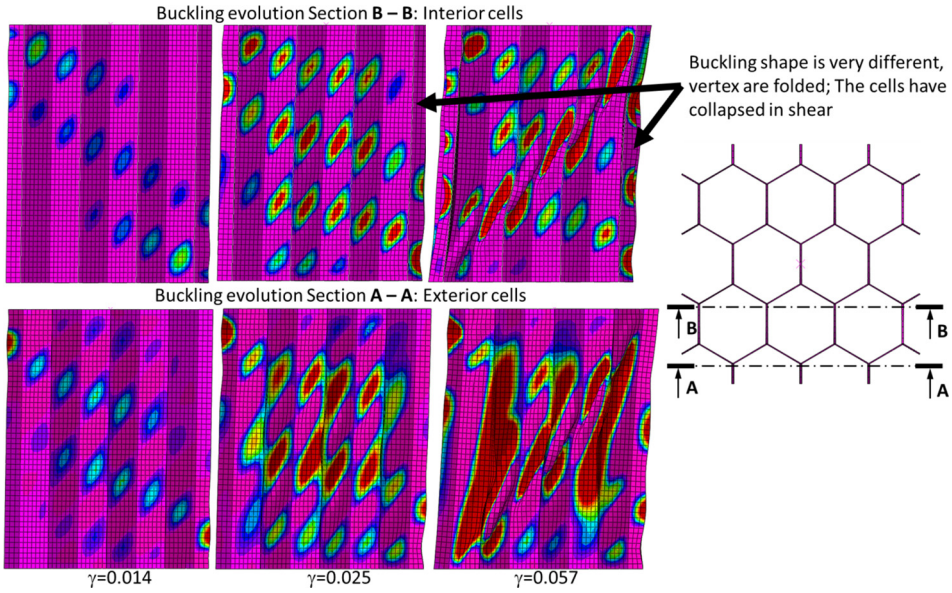

Fig. 21. Cell buckling experienced by the exterior and the interior of the specimen of the double lap test.

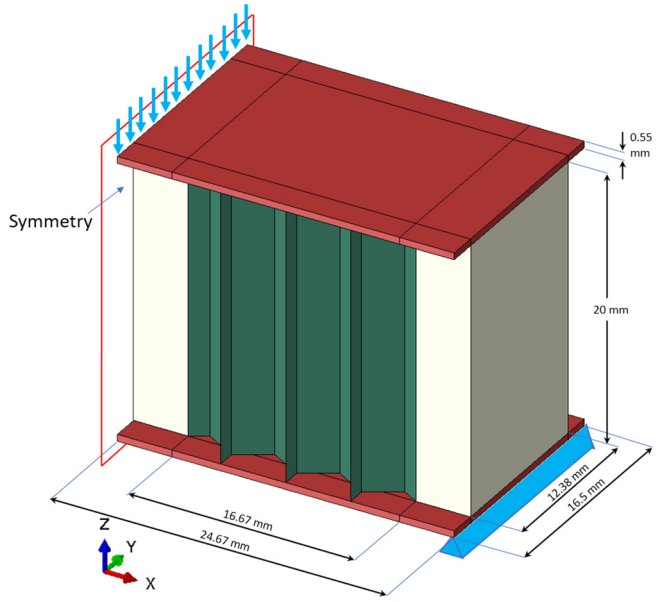

Fig. 22. Characteristics of the model of the sandwich beam with potting resin at the borders.

different buckling modes observed between classical double lap or double rail shear tests and the pull-out of inserts.

4. Influence of the boundary conditions

To better understand the differences between buckling in the rail test and in the insert pull out test (see Fig. 1), we study four cases of F.E. models with different boundary conditions. Only the W direction is analysed numerically. Then, six tests of sandwich beams with similar boundary conditions to those of the insert pull out test are presented. Finally, the analysis and the results are discussed.

4.1. Finite element analysis of the boundary conditions on the honeycomb cells

4.1.1. Case one: double lap test (reminder)

The model of the double lap test for shear testing of honeycomb core was presented in the previous section. A difference between buckling inside and on the outside of the specimen can be seen in Fig. 21. The pattern is similar but the exterior cells are slightly more folded toward the inside of the structure, which could be due to the fact that the ends of the exterior cells are free. There is a diagonal folding that starts to appear after the maximum shear stress is reached in both interior and exterior cells.

4.1.2. Case two: sandwich beam with potting resin at the borders in a three-point bending test

Regarding the boundary conditions of the insert pull-out test, an inward force was applied perpendicular to the sandwich panel surface and the skins allowed the panel to be deformed in this direction. Also, the potting blocked the displacement and rotation of the cells adjacent to it. In this sense, a three-point sandwich beam test could be considered similar to the insert pull out test as it allowed deformation of the skins in the displacement direction. To include the clamping effect of the potting in the beam specimen, the cells of the middle and the extremities of the sandwich beam were filled with potting resin. It was assumed that putting the potting at the extremities and in the middle of the sandwich beam would create similar conditions in all the cells.

An F.E. model of the sandwich beam with potting was created using Abaqus implicit (see Fig. 22). The mechanical properties of the Nomex paper were the same as for the double lap tests. The number of cells was 3 × 3 (as for the model of the double lap test). The mechanical properties of the skins were set to be similar to those of G939 woven plies: $E_x = E_y = 51{,}169$ MPa, $E_z = 5000$ MPa, $\nu_{xy} = 0.09$, $\nu_{zx} = \nu_{yz} = 0.29$, $G_{xy} = 32{,}400$ MPa, $G_{xz} = 3500$ MPa, $G_{yz} = 3500$ MPa. The potting was considered as an isotropic material with $E_x = E_y = E_z = 1300$ MPa [5]. The honeycomb cells and the skins were bonded using shell to solid coupling. The rest of the coupled instances were bonded using tie constraints. Symmetry conditions were set at the middle of the beam to simplify the calculations. A displacement of 2 mm in the Z direction was imposed in the middle of the beam and the displacement of the lower border of the sandwich was blocked in the Z direction to simulate a simple support as shown in Fig. 22.

First, a buckling analysis was performed to determine the buckling modes of the structure, which were then incorporated into the model as initial imperfections for the analysis of the post buckling behaviour of the structure.

The buckling of the cells was very different in at the outside of the specimen and inside it (see Fig. 23). The exterior cells buckled towards

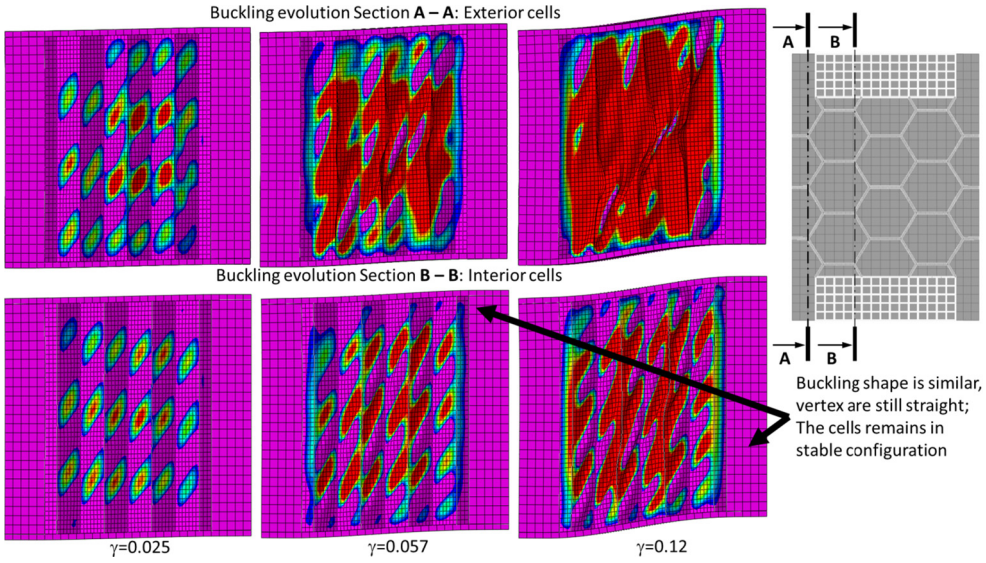

Fig. 23. Buckling of the cells at the exterior of and inside the sandwich beam with potting resin at the borders.

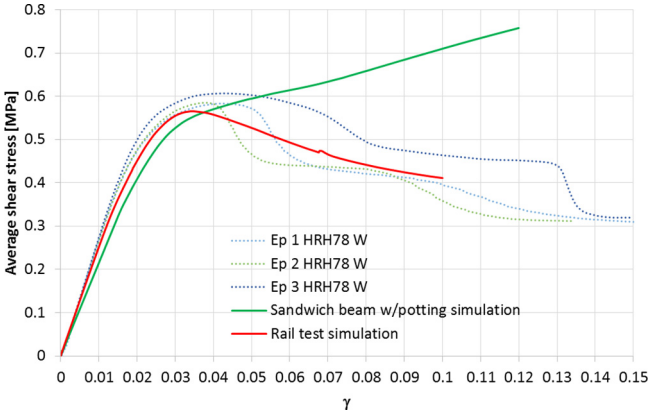

Fig. 24. Average shear stress vs γ: double lap tests and sandwich beam with potting at the borders.

the interior of the structure and collapsed, similarly to their behaviour in the rail test while, in the interior, the buckling pattern of cells kept a stabilized shape even when the displacement was large. This may have been due to the exterior cells having free borders while the interior cells were stabilized by their neighbours. For the section B-B (Fig. 23), the buckling of the cells was mostly uniform, occurring at three to four places in each cell wall.

The average γ deformation of the honeycomb core was not easy to calculate because the deformations of the skins were not uniform [5,6]. However, an approximation was obtained by neglecting the curvature of the skins. The average shear stress was obtained by dividing the force by the projection of the cells and the potting. The resulting curve is shown in Fig. 24.

The average shear modulus of the core in the FE model was a little smaller than in the experimental test because of the Saint-Venant effects of the potting. The potting simply created a more rigid boundary condition, allowing the honeycomb structure to tolerate higher loads. It was also noticeable that the global response of the honeycomb with such a boundary condition was similar to the nonlinear law used by Bunyawanichakul [5,6] for the modelling of inserts, which is more relevant.

An analysis of the rotation of the nodes of the honeycomb showed that the buckling configuration of the cells was more stable than in the rail tests, as the bifurcation point was slightly higher (Fig. 25). Also, the sandwich configuration with the potting apparently avoided the collapse of the cells by collapsing the vertical edges. In Fig. 23, the vertical edge remains almost straight, which is also consistent with the pattern obtained after a pull-out test on an insert (Fig. 1 and [5,6]). However, since only the plasticity and not the tearing of the Nomex paper were considered in the model, the results are yet to be validated and compared to a real test.

4.1.3. *Case three: honeycomb with potting and without skins*

To study the importance of the skins of the sandwich for the buckling of the cells, the skins were removed from the model of Case two. Instead of a simple support, the potting resin was clamped; no rotation or displacement was allowed. As for the previous model, symmetry was used to simplify the calculations. A displacement of 2 mm was imposed on the upper surface of the middle potting. The same method of postbuckling analysis was followed as for the other models (see Fig. 26).

The simulation showed that the core without the skins buckled in a totally different way in comparison with the previous models. There was no local buckling of the honeycomb walls. Instead, the whole honeycomb structure buckled rather like an accordion. The average shear stress vs γ curve was extracted using the same procedure as for Case two. The measured average shear modulus and core strength were very small in comparison to the manufacturer's data, as can be seen in Fig. 27.

4.2. *Shear testing with inserts, skins and vertical loading*

The numerical study pointed out that the presence of a lateral stabilization (such as an insert) combined with the stabilization provided by the skins could increase the shear strength of the honeycomb core as the cells were more stable. Also, it was shown that the buckling of the interior and exterior cells was different, as the interior cells were also stabilized by the adjacent cells. This effect was particularly accentuated when the lateral stabilization was present. Nevertheless, these conclusions were obtained by an F.E. analysis with several assumptions - as usual. To validate such conclusions, tests on the real materials under the considered boundary conditions are reported below.

Six test specimens (three in the W and three in the L direction) that were similar to those of Case two were made and tested. Knowing that the lateral stabilization had more influence on the interior cells, the specimen was made 7 cells thick. All dimensions are shown in Fig. 28.

The skins were made of G939 prepreg that was 0.275 mm thick. Two layers were used for the skins (oriented at 0°), so the total

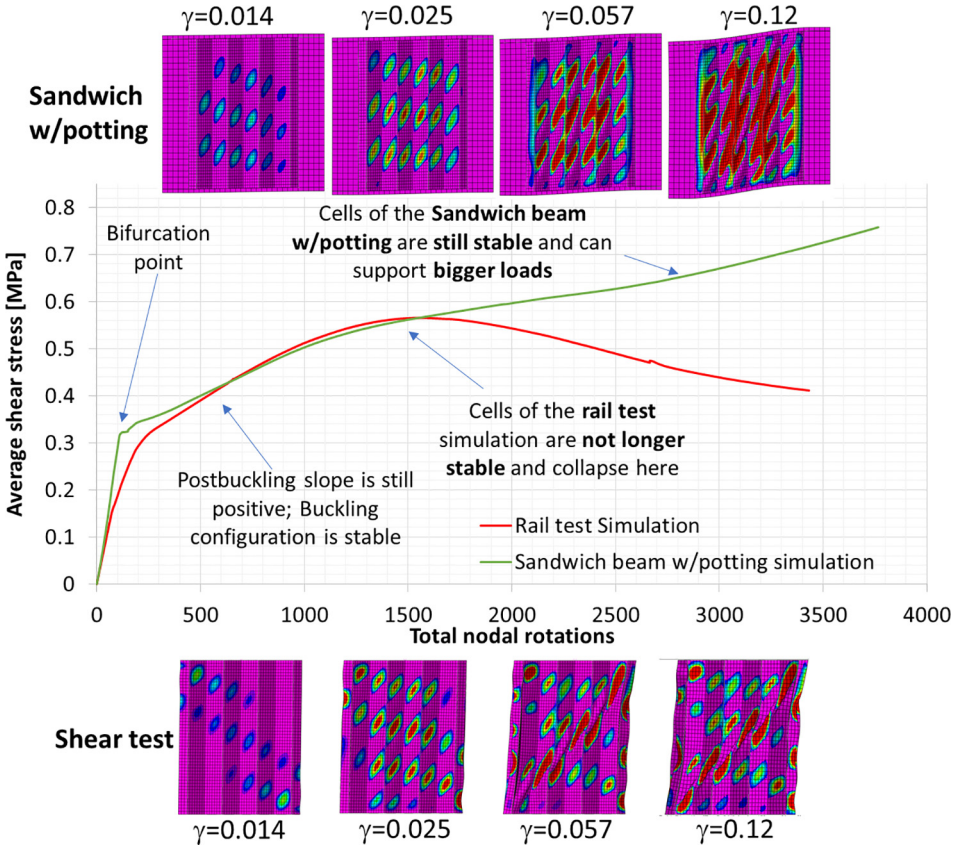

Fig. 25. Average shear stress vs total nodal rotation of the elements: Double lap tests vs sandwich beam with resin at the borders.

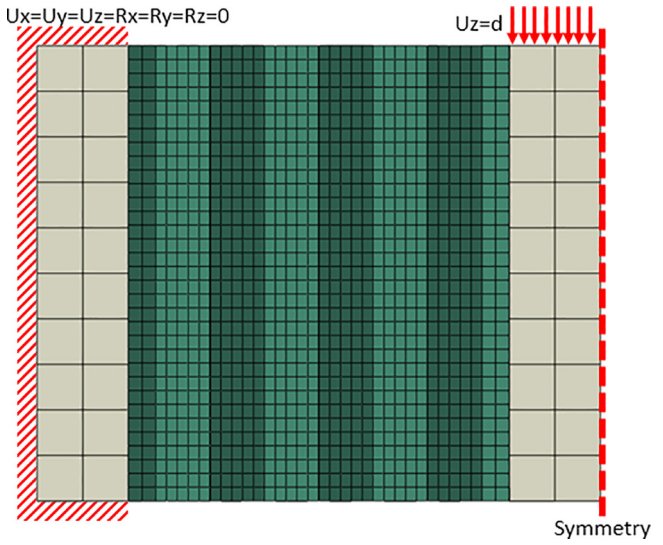

Fig. 26. Characteristics of the model of the honeycomb core without skins.

thickness was 0.55 mm. The HRH-78 Nomex honeycomb core used here was the same as in the previous tests. The potting used araldite resin AV121 B mixed with 10 percent of micro balloons as indicated in Ref. [36]. The skins were bonded using Redux 609 epoxy adhesive film, two steps being used to avoid dripping of the glue.

The supports of the beam were 150 mm apart. To measure the displacement of the skins, four small squares of glue were formed in the skins as shown in Fig. 29, then the specimens were painted with a speckle pattern on one side to measure the displacements of the skins. The imposed displacement was measured with a 3D DIC system and an LDVT sensor. One photograph was taken every 600 ms. The buckling of the exterior cells was not analysed because the main concern of the study was to determine whether the honeycomb core could tolerate higher loads if it was stabilized by the potting. An Instron 10 kN machine was used to test the specimens: a displacement of 1 mm/min was imposed and the force was measured directly by the machine. The average shear stress and γ were measured as in the study of Case two, the flexural deformation of the skins being neglected.

The beams failed at only one side (Fig. 29), so it was difficult to measure the average post failure behaviour of the honeycomb core as only one side of the specimen was filmed.

The maximum shear stresses for the W specimens were 0.63, 0.64 and 0.62 MPa for EP13, EP14 and EP15 respectively. The average value was 0.63 MPa.

The maximum shear stresses for the L specimens were 1.0607, 0.9830 and 1 MPa for EP16, EP17 and EP18 respectively. The average value was 1.0145 MPa.

According to the manufacturer, the shear strength was 0.55 and 0.855 MPa for the W and L directions, respectively. The tests revealed that the shear strength increased by 15% compared to the values given by the manufacturer and 8% compared to the values found in rail tests for the W direction. For the L direction, there was an increment of 18.6% compared to the manufacturer's values and 35% compared to the rail tests presented previously (see Figs. 30 and 31).

Thus, the tests confirmed that the honeycomb core could support more shear stress when the insert and the skin were present. Nevertheless, this result needs to be confirmed by a larger number of tests.

4.3. *Discussion of shear allowables for insert sizing*

The analyses presented so far in this section show the strong influence of boundary conditions on the buckling loads and mode of the cells. Since the boundary conditions of the core for the double lap shear

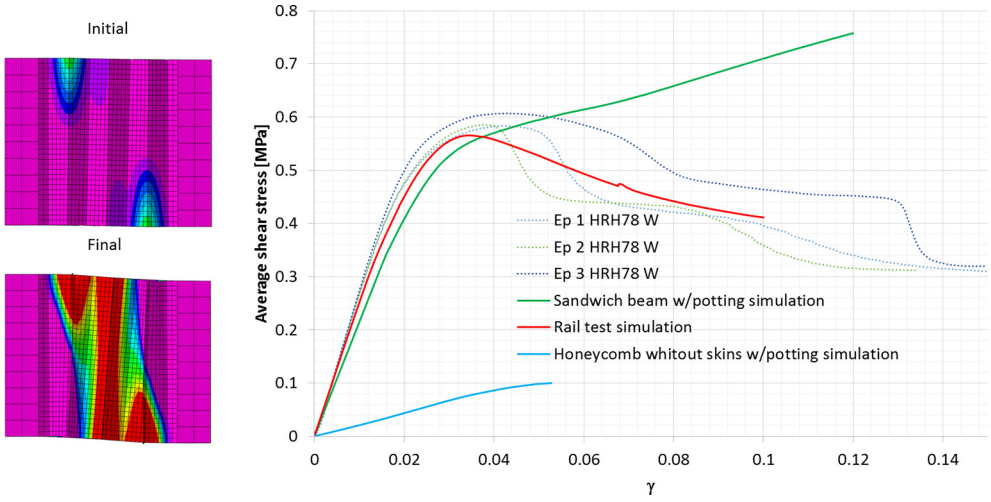

Fig. 27. Buckling of the cells and the average shear stress vs γ: three cases.

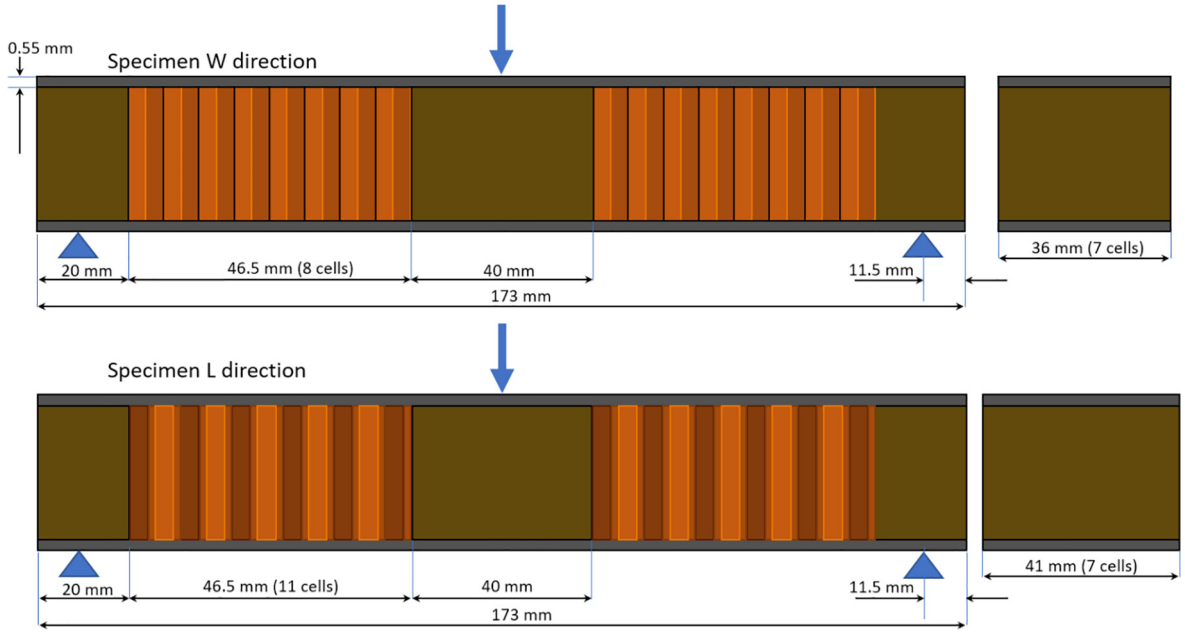

Fig. 28. Characteristics of sandwich beam specimens with potting at the borders.

or double rail shear tests (known as classical tests), are very different from those of the cells near an insert, the strength allowables for both cases should also be very different. In addition, based on the present work, it can be said that the shear strength values obtained by a rail test should not be directly used for insert sizing analytical formulas since the strength of the insert is judged to be directly proportional to the shear strength of the core. In other words, the strength of the insert should be proportional to the shear strength of the core when it is laterally stabilized by the potting. If it is chosen in any other way, the allowable of the insert is underestimated. There are several publications about insert design. Mostly, the dimensioning of inserts is obtained by analytical approaches that rely on the elastic shear properties of the honeycomb core [46,47]. A general method is also provided in the ESA Insert design book [48], where the effective strength of the core is 1.36 times the shear strength of the core in the W direction. According to the design book, this is intended to consider the effect of the number of foils in the W and L directions. Although this factor is not very clear, it supports the fact that the strength of inserts should be higher than that calculated by considering only the shear strength in the W direction (obtained mostly by a rail tests). In contrast, the present research may indicate that this effective shear strength should be about 1.16 times the shear strength in the W direction (see Fig. 30) and that it is not related to the foils in the W and L directions but to the lateral stabilization provided by the potting over the honeycomb cells.

Heimbs et al. [31] performed several pull-out test on inserts and found that using the analytical approach of ESA without considering the effective shear strength correction factor led to an underestimation of the strength of the inserts by 23%. If the ESA correction factor of 1.36 is used, the strength of the insert is overestimated by 18.8%. In contrast, if the correction factor found this research is used (1.16 instead 1.36), the shear strength is overestimated by 0.45%. When this same comparison procedure was applied to the inserts tested in the works of Kumsantia [50], Roy et al. [30], Bunyawanichakul et al [6] and Song et al. [49], the overestimation errors using the correction factor of ESA (1.36) were 23.29%, 21.12%, 32.63% and 18.91% respectively. When the correction factor of this research was used (1.16) the errors where 4.25%, 2.42%, 12.15%, and 0.55% respectively. These much smaller discrepancies may indicate that this research could be very useful to explain and understand the errors of insert sizing methods.

ESA recommends testing the inserts in all cases, as the best method

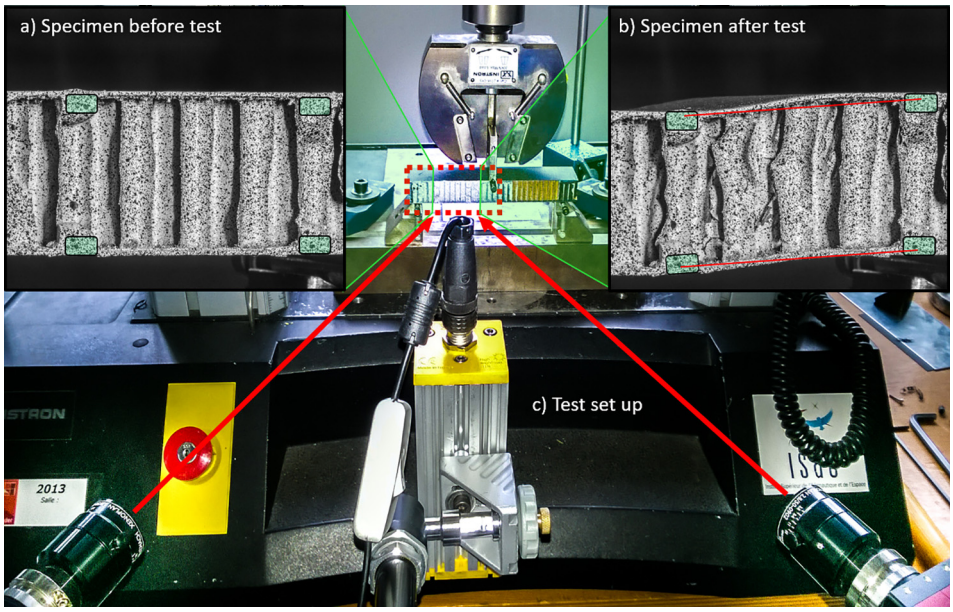

Fig. 29. Testing of the sandwich beam specimens with resin at the borders, before and after the tests.

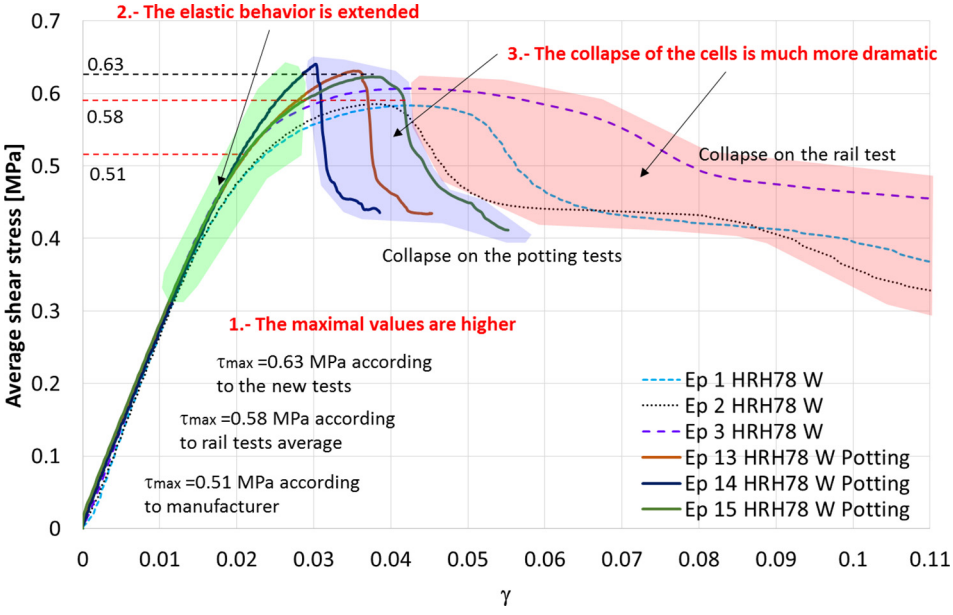

Fig. 30. Curves of the double lap tests for the sandwich beam with potting at the borders (W-Direction).

to determine their strength (as Song et al. did in Ref. [49]). However, this is not an approach that allows the properties of the insert to be predicted properly. Other methods based on F.E. modelling have been developed to reduce the oversizing of inserts. In Refs. [5,6] Bunyawanichakul et al. developed an insert model based on the nonlinear behaviour of the materials of the insert and the model was better able to capture the failure scenario. For insert design, the parameters that the designer may modify are only the radius and the potting material, as the thicknesses of the skins and the core material are selected by the main application of the sandwich panel.

In this sense, if designers tested their honeycomb materials with similar boundary conditions to those of inserts as explained above, they might find that their designs are oversized, which could lead to a reduction of the weight of the sandwich panel.

5. Conclusions

Both numerical analysis and experiments have highlighted and confirmed the different nonlinear behaviour of honeycomb under shear when different boundary conditions are used. Although it should be obvious, it is nevertheless worth recalling here that honeycomb is firstly a complex structure, so the boundary conditions have strong effects, especially for buckling and postbuckling.

The results show that the buckling of Nomex honeycomb core presents nonlinear elastic behaviour beyond the buckling point. This is due to reversible postbuckling as in aerospace structures. The incorporation of the nonlinear behaviour could be very useful for inserts, possibly corners, where the buckling point and the beginning of the nonlinear behaviour determine the allowable for the structure.

Depending on the load direction, the boundaries of the honeycomb and the size of the specimen, the failure scenarios may differ. In classical tests such as double rail shear tests or double lap shear tests, the

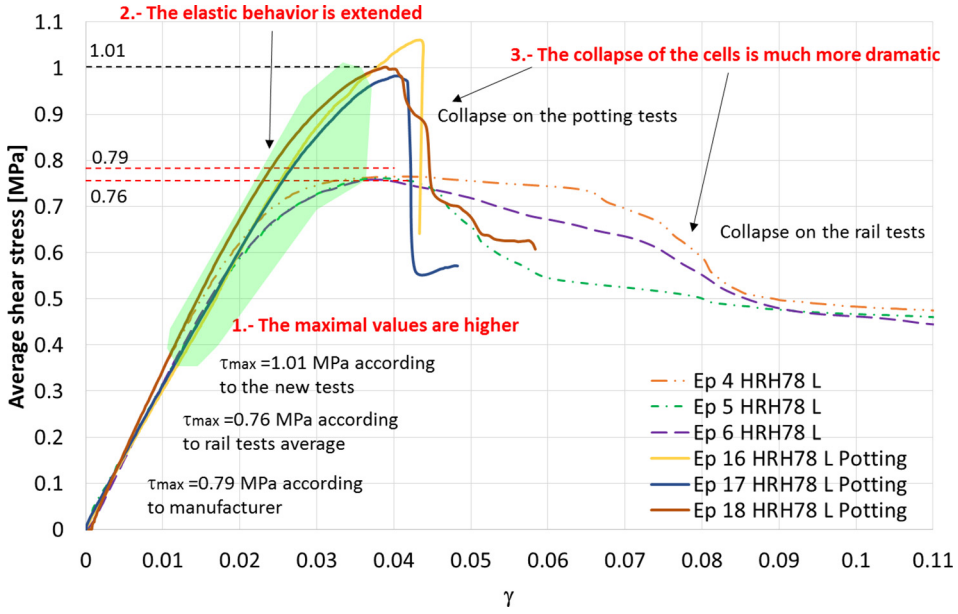

Fig. 31. Curves of the double lap tests for the sandwich beam with potting at the borders (L-Direction).

main loading direction is orthogonal to the cell edges at the vertex of the hexagonal shape. Thus, after a postbuckling regime, the honeycomb fails by collapse of these edges in shear. Although the tested specimen mimics the inserts in sandwich panels quite well, the loading direction is parallel to these cell edges and the structure tolerates the shear buckling more easily, thus generating a gain in the allowable of up to 35%.

However, the results presented in this study are preliminary ones and are limited to the case of the Nomex honeycomb used. Variability studies should be carried out for the same honeycomb and the results checked for other types of honeycomb. Moreover, the tests were performed in the L and W directions and it could be interesting to see how the core behaves out of the orthotropic axes. In addition, the fatigue response remains to be investigated in the field of post-buckling.

This nonlinear analysis will also be useful to develop a damage model of honeycomb and an enhanced nonlinear insert model.

Acknowledgments

The present work was supported in part by the Mexican government through the programme “Becas Conacyt- Gobierno Frances” and the Institut Clement Ader. This support is acknowledged with gratitude. The authors also wish to thank SOGECLAIR Aerospace for its support, especially J.P. Giavarini and M. Deloubes.

References

[1] Kassapoglou C. Design and analysis of composite structures (with applications to aerospace structures). Wiley; 2010.
[2] Zenkerts D. The handbook of sandwich construction. EMAS Publishing; 1995.
[3] Gay D. Composite materials: design and applications. CRC Press; 2014.
[4] Seemann R, Krause D. Numerical modeling of Nomex honeycomb sandwich cores at meso-scale level. Compos Struct 2017;159:702–18.
[5] Bunyawanichakul P, Castanié B, Barrau JJ. Non-linear finite element analysis of inserts in composite sandwich structures. Compos Part B 2008;39(7–8):1077–92.
[6] Bunyawanichakul P, Castanié B, Barrau JJ. Experimental and numerical analysis of inserts in sandwich structures. Appl Compos Mater 2005;12(3–4):177–91.
[7] Mezeix L, Dols S, Bouvet C, Castanié B, Giavarini J-P, Hongkarnjanakul N. Experimental analysis of impact and post-impact behaviour of inserts in Carbon sandwich structures. J Sand Struct Mater, on line. http://dx.doi.org/10.1177/1099636216687582.
[8] ASTM C273: Standard Test Method for Shear Properties of Sandwich Core Materials; 2007.
[9] Chen Y, Das R, Battley M. Response of honeycombs subjected to in-plane shear. J Appl Mech 2016;83(6):061004.
[10] Grediac M. A finite element study of the transverse shear in honeycomb cores. Int J Sol Struct 1993;30(13):1777–88.
[11] Chenand DH, Ozaki S. Analysis of in-plane elastic modulus for a hexagonal honeycomb core: effect of core height and proposed analytical method. Compos Struct 2009;88(1):17–25.
[12] McFarland RK. Hexagonal cell structures under post-buckling axial load. AIAA J 1963;1(6):1380–5.
[13] Wierzbicki T. Crushing analysis of metal honeycomb. Int J Impact Eng 1983;1(2):157–74.
[14] Wu E, Jiang WS. Axial crush of metallic honeycomb. Int J Impact Eng 1997;19(5–6):439–56.
[15] Zhao Y, Sun Y, Li R, Sun Q, Feng J. Response of aramid honeycomb sandwich panels subjected to intense impulse loading by Mylar flyer. Int J Impact Eng 2017;104:75–84.
[16] Navarro P, Marguet S, Ferrero JF, Barrau JJ, Lemaire S. Modelling of impacts on sandwich structures. Mech Adv Mater Struct 2012;19(7):523–9.
[17] Abrate S, Castanié B, Rajapakse YDS. Dynamic failure of composite and sandwich structures. Springer; 2012.
[18] Yang M, Qiao P. Quasi-static crushing behavior of aluminum honeycomb materials. J Sand Struct Mater 2008;10:133–60.
[19] Aktay L, Johnson AF, Kroplin BH. Numerical modelling of honeycomb core crush behaviour. Eng Fract Mech 2008;75:2616–30.
[20] Heimbs S. Virtual testing of sandwich core structures using dynamic finite element simulations. Compos Mater Sci 2009;45:205–16.
[21] Giglio M, Manes A, Gilioli A. Investigations on sandwich core properties through an experimental–numerical approach. Compos Part B 2012;43:361–74.
[22] Aminanda Y, Castanié B, Barrau JJ, Thevenet P. Experimental analysis and modeling of the crushing of honeycomb cores. Appl Compos Mater 2005;12(3–4):213–7.
[23] Castanié B, Bouvet C, Aminanda Y, Barrau JJ, Thevenet P. Modelling of low energy/low velocity impact on Nomex honeycomb sandwich structures with metallic skins. Int J Impact Eng 2008;35:620–34.
[24] Castanié B, Aminanda Y, Bouvet C, Barrau JJ. Core crush criteria to determine the strength of sandwich composite structures subjected to compression after impact. Compos Struct 2008;86:243–50.
[25] Zhang J, Ashby MF. The out-of-plane properties of honeycombs. Int J Mech Sci 1992;34(6):475–89.
[26] Pan SD, Wu LZ, Sun YG, Zhou ZG, Qu JL. Longitudinal shear strength and failure process of honeycomb cores. Compos Struct 2006;72:42–6.
[27] Pan SD, Wu LZ, Sun YG. Transverse shear modulus and strength of honeycomb cores. Compos Struct 2008;84:369–74.
[28] Bianchi G, Aglietti GS, Richardson G. Static and fatigue behaviour of hexagonal honeycomb cores under in-plane shear loads. Appl Compos Mater 2012;19:97–115.
[29] Gornet L, Marguet S, Marckmann G. Modeling of Nomex honeycomb cores, linear and nonlinear behaviors. Mech Adv Mater Struct 2007;14:1–13.
[30] Roy R, Nguyen KH, Park YB, Kweon JH, Choi JH. Testing and modeling of Nomex™ honeycomb sandwich Panels with bolt insert. Compos Part B 2014;56:762–9.
[31] Heimbs S, Pein M. Failure behaviour of honeycomb sandwich corner joints and inserts. Compos Struct 2009;89(4):575–88.
[32] Roy R, Park YB, Kweon JH, Choi JH. Characterization of Nomex honeycomb core constituent material mechanical properties. Compos Struct 2017;117(1):255–66.
[33] Serra J, Pierré JE, Passieux JC, Périé JN, Bouvet C, Castanié B. Validation and modeling of aeronautical composite structures subjected to combined loadings: the VERTEX project. Part 1: experimental setup, FE-DIC instrumentation and procedures. Compos Struct 2017;179:224–44.
[34] Serra J, Pierré JE, Passieux JC, Périé JN, Bouvet C, Castanié B, et al. Validation and

modeling of aeronautical composite structures subjected to combined loadings: the VERTEX Project. Part 2: load envelopes for the assessment of panels with large notches. Compos Struct 2017;180:550–67.
[35] Barrière L, Marguet S, Castanié B, Cresta P, Passieux JC. An adaptive model reduction strategy for post-buckling analysis of stiffened structures. Thin-Walled Struct 2013;73:81–93.
[36] Bunyawanichakul P. Contribution à l'analyse du comportement des inserts dans les structures sandwichs composites. PhD Supaéro; 2005. https://depozit.isae.fr/theses/2005/2005_Bunyawanichakul_Phacharaporn.pdf.
[37] HexWeb. HexWeb honeycomb attributes and properties. 1999.
[38] Giglio M, Manes A, Gilioli A. Numerical investigation of a three point bending test on sandwich panels with aluminum skins and Nomex™ honeycomb core. Compos Mater Sci 2012;56:69–78.
[39] ASTM C393/C393M-16 Standard Test Method for Core Shear Properties of Sandwich Constructions by Beam Flexure; 2011.
[40] Hodge AJ, Nettles AT. A novel method of testing the shear strength of thick honeycomb composites: NASA Technical Paper 3108. 1991.
[41] Tsujii Y, Tanaka K, Nishida Y. Analysis of mechanical properties of aramid honeycomb core. Trans Jpn Soc Mech Eng 1995;61(587):1608–14.
[42] Foo CC, Chai GB, Seah LK. Mechanical properties of Nomex material and Nomex honeycomb structure. Compos Struct 2007;80(4):588–94.
[43] Fischer S, Drechsler K, Kilchert S, Johnson A. Mechanical tests for foldcore base material properties. Compos Part A 2009;40(12):1941–52.
[44] Hexcel Composites. HRH-78 Nomex commercial grade honeycomb product data. 1998. p. 6–9.
[45] Bitzer T. Honeycomb technology: materials, design, manufacturing, applications and testing. 1997.
[46] Bozhevolnaya E, Lyckegaard A, Thomsen OT, Skvortsov V. Local effects in the vicinity of inserts in sandwich panels". Compos Part B 2004;35(6–8):619–27.
[47] Thomsen OT. Sandwich plates with 'through-the-thickness' and 'fully potted' inserts: evaluation of differences in structural performance. Compos Struct 1997;40(2):159–74.
[48] ECSS. Insert design handbook March 2011. p. 488.
[49] Song KI, Choi JY, Kweon JH, Choi JH, Kim KS. An experimental study of the insert joint strength of composite sandwich structures. Compos Struct 2008;86(1–3):107–13.
[50] Bunyawanichakul P, Kumsantia P, Castanié B. An experimental-numerical approach of the metallic insert in CFRP/honeycomb sandwich structures under normal tensile load. Adv Mater Res 2012;399–401:500–5.